TYCO LABORATORIES, INC.
BEAR HILL, WALTHAM 54, MASSACHUSETTS
AREA CODE 617
TELEPHONE: 899-1650

RESEARCH RELATING TO FUEL CELLS

The Oxygen Reaction on Platinum and Gold in Acid Solutions

A. K. M. Shamsul Huq
Principal Investigator

Final and Summary Report
Covering Period October 1, 1961 to February 28, 1963
Contract DA-49-186-ORD-982

414800

April 1, 1963
Prepared for:
HARRY DIAMOND LABORATORIES
ORDTL-940-25

TABLE OF CONTENTS

I. ABSTRACT

The electrode kinetics of the oxygen reaction were studied on smooth platinum and gold electrodes in acid solutions (H_2SO_4 and $HClO_4$) and at room temperature. Polarization curves were obtained both galvanostatically and at controlled potentials. The electrode coverage by adsorbed oxygen and the extent of oxide formation were determined using chronopotentiometry and potentiostatic sweep methods. The kinetics of the electrochemical reduction and oxidation of hydrogen peroxide, an intermediate found in solution during the reduction of oxygen, were also studied.

Platinum forms a thin oxide at potentials where oxygen evolution takes place. The rate-determining reaction in oxygen evolution is the discharge of a water molecule which occurs with a Tafel slope of 0.086 V (transfer coefficient, $\alpha \sim 0.7$). On cathodized (reduced) Pt surfaces, the discharge of water occurs at a higher rate than on superficially oxidized surfaces. The transfer coefficient ($\alpha = 0.45$) on cathodized surfaces corresponds to a nearly symmetrical energy barrier.

Reduction of oxygen on Pt electrodes proceeds through the formation of peroxide, which can be reduced to H_2O electrochemically. Rapid, galvanostatic measurements under conditions where the H_2O_2 concentration in solution is negligible, suggest that the rate-determining step is either the reduction of oxygen to O_2^- (or HO_2) or the direct, two-electron reduction of O_2 to HO_2. Steady-state, potentiostatic measurements show that in the over-all reduction of oxygen to water, the slow step is the discharge of H_2O_2 which occurs with a Tafel slope of 0.085 V ($\alpha \sim 0.7$).

The rest potential of platinum electrodes in nitrogen-saturated, H_2O_2 solutions is independent of the peroxide concentration but changes with pH according to $(\partial E / \partial pH) = -0.043$ V. The electrochemical reaction order both for reduction and oxidation of H_2O_2 is unity in strongly acid solutions. The rest potential in peroxide solutions is a mixed potential and is determined by the reactions

$$H_2O_2 + 2H^+ + 2e_o^- \longrightarrow 2H_2O \qquad E_o = 1.77\ V \quad (1)$$

and $$H_2O_2 \longrightarrow O_2 + 2H^+ + 2e_o^- \qquad E_o = 0.682\ V \quad (2)$$

Gold forms a surface oxide, probably Au_2O_3, above 1.35 V but is essentially free of adsorbed oxygen or of oxide at all potentials below 1.25 V. Oxygen evolution on essentially oxide-free electrodes proceeds at a rate which is several orders of magnitude greater than on oxide-covered electrodes. The Tafel slope, 0.125 V, suggests that the rate-determining step is the discharge of a water molecule on both oxide-free and superficially oxidized electrodes.

Oxygen reduction on gold generally shows two clearly defined regions, one at potentials above 0.7 V and the other at potentials below 0.5 V. The current in the transition region is approximately independent of the potential although it is not diffusion-limited (since it is not dependent on stirring). This result suggests that a change in mechanism takes place as the potential becomes more negative. The reduction process probably involves a chemical decomposition of an adsorbed intermediate, most likely H_2O_2 to water, which is not dependent on potential. At high overpotentials (nine negative potentials), the electrochemical reduction of H_2O_2 according to

$$M - O_2H_2 + H^+ + e_o^- \longrightarrow M - OH + H_2O$$

is probably the slow step; the subsequent electrochemical reduction of the adsorbed hydroxyl radical, produced in the above step, according to

$$M - OH + H^+ + e_o^- \longrightarrow M + H_2O$$

is probably rapid.

H_2O_2 is found in solution during O_2 reduction on gold, but in smaller concentration than with Pt electrodes under comparable conditions. The rest potential of gold in nitrogen-saturated, H_2O_2 solutions is independent of the H_2O_2 concentration. However, the rates of oxidation and of reduction of H_2O_2 are first order with respect to peroxide concentration. Therefore, it appears that the rest potential of gold electrodes in H_2O_2 solutions is a mixed potential, as it is on Pt electrodes, and is determined by reactions (1) and (2) given above. The rate of the oxidation reaction of H_2O_2 is also dependent on the state of the electrode surface and is slower on oxidized than on reduced surfaces by an order of magnitude.

II. INTRODUCTION

The objective of the present program was the theoretical and experimental investigation of the mechanism of the oxygen reaction in aqueous solutions. The electrochemical oxidation of water and the reduction of oxygen are complicated by the formation of surface oxides or of chemisorbed layers of oxygen, by the production of stable intermediates which participate in side reactions, and by adsorption of anions at the high positive potentials at which these reactions take place. The electrodes chosen for these studies were among those expected to show relatively simple behavior. In particular, it was desirable to avoid side reactions involving extraneous redox couples, e. g., corrosion reactions. It was also desirable to work with electrodes which did not form thick oxide films, i. e., passive films, at the relevant potentials. Platinum and gold were selected for these reasons and also because of other known specific properties of these metals. Platinum is a good catalyst for a wide variety of electrochemical reactions; gold is the only metal which is thermodynamically stable with respect to oxidation in air at room temperature[1] and is one of the very few metals which do not chemisorb oxygen at room temperature[2].

The general approach to the experimental study of oxygen reduction on Pt and Au was to obtain steady-state polarization curves in aqueous solutions of H_2SO_4 and $HClO_4$ saturated with oxygen and to compare these with similar curves obtained in nitrogen- or in argon-saturated solutions. Since the oxygen reaction is highly irreversible, and the current on smooth electrodes is small at potentials close to the reversible potential, it was necessary to work with highly purified solutions. In addition, the residual current in the absence of oxygen was measured directly in order to have a check on the accidental presence of other redox couples (impurities) which could lead to erroneous results. Most steady-state measurements were carried out potentiostatically, an experimental method which proved generally superior to galvanostatic measurements for this particular reaction.

Polarization measurements were also carried out in aqueous acid solutions containing hydrogen peroxide, a stable intermediate found in the solution during oxygen reduction on both Pt and Au electrodes. Finally, potentiostatic sweep and galvanostatic charging curves were obtained in order to characterize the electrode surface at various potentials within the range traversed in the steady-state polarization measurements.

III. EXPERIMENTAL

A. THE ELECTROLYTIC CELLS

Cells of three different designs were used. They were all Pyrex, three-compartment cells with provisions for minimizing liquid diffusion between compartments. In the earliest design, the electrodes were mounted through windows onto the walls of the working electrode compartment by means of Teflon O-rings. The electrodes were circular platinum discs and had one face exposed to the electrolytic solution. Solutions were prepared by directly distilling water into a preparation vessel which also served as the pre-electrolysis vessel. The electrolytic cell was first rinsed thoroughly by pre-electrolyzed solution which was pushed into this cell by gas pressure.

Certain new features were introduced in a subsequent design which allowed four fresh electrodes to be examined in a single run, and pre-electrolysis of the solution to be performed in the cell itself. In these series of experiments, the electrode surface was exposed to the solution only during the time polarization measurements were being performed. Electrodes, usually circular discs, were spot-welded to a short length of platinum wire which was then sealed onto a Pyrex support. The Pyrex support moved within a second tube which was sealed onto the cell. Each electrode was immersed in the solution just prior to a run and was withdrawn at the end of the run. The reference electrode was a platinized platinum hydrogen electrode.

Most of the experiments on gold were performed in the third cell which is shown in Fig. 1-A. The electrodes, in the shape of cylinders, were mounted by a method described by Stern and Makrides[3], so that only Teflon and Pyrex glass (in addition to the electrode) were exposed to solution.

B. SOLUTION PREPARATION AND CLEANING OF APPARATUS

All chemicals were of Analytical Reagent Grade and were used without further purification. Initially, all solutions were subjected to

pre-electrolysis. It was subsequently found that pre-electrolysis made no essential difference in the measurements, provided proper care was taken during the preparation of the experiments. Fresh conductivity water was used to make up solutions and to wash the apparatus. The distillation of water was performed in four stages, viz., from a commercial distillation unit to a tin-lined, precision still to which permanganate had been added, and finally to a two-stage quartz still.

All glass apparatus was immersed in chromic-sulfuric acid cleaning mixture for several hours, or overnight, and thoroughly washed with triply distilled water (no tap water being used at any time).

C. THE GAS PURIFICATION TRAIN

Oxygen gas obtained from commercial tanks was purified through a conventional purification train shown in Fig. 1-B. The gas was passed through a copper oxide furnace at 450°C, a palladized asbestos furnace at 450°C, tubes containing silica gel and soda lime, and finally through three liquid oxygen cold traps containing crushed Pyrex glass. The purified gas was then distributed through a manifold. Nitrogen was purified by a similar train with liquid N_2 in the cold traps. A flowmeter was used in the train to monitor the rate of gas bubbling in the cell. Hydrogen, used in the reference electrode compartment was passed first through a liquid nitrogen trap.

D. ELECTRODE PREPARATION

All platinum samples were C. P. Grade (99.8% guaranteed purity), and all gold samples were spectroscopically pure grade obtained from three different sources. Platinum disc electrodes (0.5 - 3 cm^2) were mechanically polished to remove gross surface irregularities and finally polished with alumina to a high finish. The electrodes were treated ultrasonically in distilled water to remove any adhering particles and were then annealed in air for about 15 hours at 500°C in a muffle furnace. They were treated with chromic-sulfuric acid mixture and thoroughly washed

with distilled water before mounting in the cell.

Gold electrodes were in the form of circular discs (thickness - 20 mils; area - 2 cm^2) and of cylinders (diameter - 0.3 cm; area - 0.9 cm^2). The disc electrodes were mounted through a short length of a platinum wire which was gold-plated after sealing into the usual glass support. The cylindrical samples were mounted by the method mentioned above[3]. The gold electrodes were mechanically polished to a high finish, treated with chromic-sulfuric acid mixture and washed thoroughly with triply distilled water. Alternately, mechanically polished electrodes were electropolished using the method presented by McG. Tegart[4], cleaned in chromic-sulfuric acid, and washed with triply distilled water.

E. ELECTROCHEMICAL MEASUREMENTS

Constant current measurements were carried out using a bank of batteries (135 V) and external resistances which exceeded the cell resistance by at least two orders of magnitude. Currents were measured with a micro-milliammeter to 1/2% accuracy. Potentials were measured with a Sargent MR Recorder using a high impedance circuit (current drain $< 10^{-13}$ A).

Potentiostatic measurements were carried out with a Wenking, high-speed potentiostat. Potential sweep measurements were made using this potentiostat and a triangular wave generator (Hewlett-Packard). The current was recorded with a Tektronix 545 Oscilloscope (see Fig. 1-C).

IV. RESULTS

A. THE OXYGEN REACTION ON PLATINUM

1. The Oxygen Evolution Reaction (o. e. r.).

Two constant current techniques were employed to establish the Tafel relationship (overpotential vs $\log_{10}$ of current density) for the o. e. r. on Pt. In one case, the electrode was polarized at a certain high constant current density (C. D.), say 1 mA/cm^2, until the potential was essentially constant ($<$ 1 mv per min). Then the C. D. was decreased stepwise and the corresponding potentials were recorded. The potential at a given C. D. showed essentially no variation with time. The Tafel line could be recorded to a C. D. in the range 10^{-7} to 10^{-6} A/cm^2. The potentials became less anodic (depolarization) with time at smaller current densities and the Tafel relation was no longer valid. The C. D. at which the Tafel relation failed was higher for a stirred than for an unstirred solution. Evidently, depolarization was caused by diffusion of some species from the bulk of the solution to the electrode surface. A typical Tafel line is shown in Fig. 2 (curve 1). The results obtained by this technique in three independent runs, in each case using four apparently identical electrodes, are presented in Table I. The mean exchange C. D. is $i_o = 3 \times 10^{-10}$ A/cm^2 and the mean Tafel slope is 0.086 V, which corresponds to a transfer coefficient of $\alpha = 0.7$. These results compare well with b = 0.097 V and $i_o = 2 \times 10^{-10}$ A/cm^2 reported by Bockris and Huq[5] who used a similar technique. It is of interest to note that when the same electrode was used in successive runs starting from the same C. D. (3×10^{-4} A/cm^2) but waiting for longer periods at higher overpotentials, the Tafel slope remained essentially constant, but i_o decreased somewhat. Thus, the time variation of overpotential probably involves a decrease in the activity of the electrode with time, but no apparent change in the mechanism of the o. e. r.

In the second technique, the electrode was alternately subjected to anodic and cathodic polarization at the same C. D. for equal time intervals. The potential was followed with time on an MR Recorder. The intersect

TABLE I

Tafel Parameters for Steady State Anodic Polarization of Bright Pt Electrodes in 0.1 N H_2SO_4 Solution at 25°C.

b_a(mv)	-Log i_o (A/cm^2)	C. D. range (A/cm^2)
77	9.4	3×10^{-6} - 10^{-4}
71	9.6	3×10^{-6} - 10^{-4}
85	8.8	3×10^{-6} - 10^{-4}
92	9.2	3×10^{-6} - 10^{-3}
90	9.6	10^{-6} - 3×10^{-5}
95	10.0	3×10^{-6} - 2×10^{-4}
84	9.3	3×10^{-7} - 2×10^{-4}
84	9.3	3×10^{-7} - 3×10^{-4}
104	9.2	10^{-7} - 3×10^{-4}
78	10.0	10^{-6} - 3×10^{-4}
81	9.9	3×10^{-7} 10^{-4}
86	9.6	10^{-6} - 10^{-4}
Mean 86 ± 7	9.5 ± 0.3	
$\alpha = 0.7$		

of the linear extrapolations of the sharp initial rise and of the following slow increase of the potential (see Fig. 3) was taken as the overpotential free from the slow time variation effect and was used to obtain the results presented in Table II. A typical Tafel line is shown in Fig. 2 (curve II). The mean Tafel parameters are : $b = 0.133$ V, $i_o = 7.6 \times 10^{-8}$ A/cm^2 and $\alpha = 0.45$. The Tafel slope obtained by this technique is higher than that obtained by the steady state technique and i_o is about 3 orders of magnitude larger.

2. The Electrochemical Reduction of Oxygen

Both the resting potential and the current potential relationship in 0.1 N H_2SO_4 were influenced by the preceding polarization history of the electrode. Thus, after anodic polarization, the resting potential was about 80 to 100 mv more cathodic than after cathodic polarization. The Tafel lines were shifted accordingly, depending on whether the electrode had been prepolarized anodically or cathodically.

In Table III are shown results obtained with electrodes which were subjected to previous cathodic polarization. The potentials attained during the prepolarization were 0.5 - 0.6 V, i.e., they were sufficiently negative so that oxides on the Pt surface are reduced. There are two sections of the Tafel line: in the C. D. range 10^{-6} -- 10^{-5} A/cm^2 the mean slope is 0.056 V and in the C. D. range 10^{-5} -- 10^{-4} A/cm^2 the mean slope is 0.108 V. The deviations in the values of the slopes are considerable.

The results on electrodes previously subjected to anodic polarization appear to vary considerably from run to run. However, the following characteristics are observed. If a quick cathodic run is made (after the potential has decayed to a resting value on interruption of the anodic prepolarization current), a straight Tafel line is obtained with a slope of about 0.035 V in the C. D. range 10^{-6} -- 10^{-4} A/cm^2. Some typical results on four apparently identical electrodes from a single run are

TABLE II

Tafel Parameters for Anodic Polarization Alternate with Cathodic Polarization at the Same C. D. in 0. 1 N H_2SO_4 at 25°C

b_a(mv)	-Log i_o (A/cm^2)	C. D. Range (A/cm^2)
138	7. 0	10^{-5} 10^{-3}
127	7. 1	2×10^{-5} - 7×10^{-3}
125	7. 5	10^{-5} - 3×10^{-4}
127	7. 4	2×10^{-6} - 10^{-4}
138	7. 4	10^{-5} - 10^{-4}
141	6. 3	2×10^{-5} - 2×10^{-4}
Mean 133 $\pm$ 6	7. 1 $\pm$ 0. 3	

TABLE III

Tafel Parameters for O_2 Reduction in 0.1 N H_2SO_4 on Cathodically Prepolarized Pt Electrodes

$b_{c(1)}$ (mv)	C. D. Range (A/cm^2)	$b_{c(2)}$ (mv)	C. D. Range (A/cm^2)
48	10^{-6} - 3×10^{-5}	96	3×10^{-5} - 10^{-3}
64	10^{-6} - 3×10^{-5}	88	3×10^{-5} - 10^{-3}
64	6×10^{-6} - 6×10^{-5}	95	6×10^{-5} - 6×10^{-4}
59	6×10^{-6} - 6×10^{-5}	100	6×10^{-5} - 6×10^{-4}
62	3×10^{-6} - 3×10^{-5}	100	3×10^{-5} - 3×10^{-4}
62	2×10^{-5} - 10^{-4}	--	--
36	3×10^{-6} - 3×10^{-5}	117	10^{-4} - 3×10^{-3}
--	--	145	10^{-6} - 2×10^{-3}
--	--	110	2×10^{-5} - 3×10^{-4}
--	--	119	10^{-5} - 3×10^{-6}
Mean 56 ± 8		108 ± 13	

presented in Table IV. In Fig. 4 are presented the Tafel lines on an electrode which was cathodically prepolarized (curve I), and on one which was anodically prepolarized (curve II).

The potential showed a characteristic time variation above a C. D. of $\sim 10^{-5}$ A/cm^2. On setting a new, higher C. D., there was overshoot of the potential followed by a slow drift to more cathodic potentials. Once this process had taken place, the electrode behaved as a "cathodically prepolarized" electrode. This transition occurred in the potential range 0.75 - 0.8 V, i.e., in the potential region where reduction of the surface oxide is evident from the charging curves (see below).

Potentiostatic Runs:

Cathodic polarization curves on bright Pt in O_2 - saturated N H_2SO_4 were also obtained potentiostatically. A typical curve is shown in Fig. 5. The Tafel slope, which is 0.080 V in the range 10^{-7} to 10^{-5} A/cm^2, does not correspond to the slopes determined by galvanostatic measurements with either cathodized or anodized electrodes. The major difference between these sets of experiments is in the time elapsed during measurement. In the potentiostatic runs, the potential was kept fixed until the current reached a steady value; this required 10 - 15 min. at each potential so that the total curve was obtained in 3 - 4 hrs. In the galvanostatic runs, the total time for obtaining a polarization curve was less than 15 min. The cause of the deviation between the two sets of data is discussed below.

3. Potentiostatic Sweep, Galvanostatic, and Potential Decay Curves

(a) The current-potential curve obtained with Pt in N H_2SO_4 as the potential is changed linearly from zero to oxygen evolution and back to zero is shown in Fig. 6. The first two current peaks are due to ionization of hydrogen. Oxygen begins to be deposited at about 0.85 V, following

TABLE IV

Tafel Parameters for Cathodic O_2 Reduction in 0.1 N H_2SO_4 on Anodically Prepolarized Pt Electrodes

b_a (mv)	C. D. Range (A/cm^2)
45	10^{-6} - 10^{-5}
30	3×10^{-7} - 3×10^{-4}
36	3×10^{-7} - 10^{-4}
35	3×10^{-7} - 3×10^{-4}
Mean 37 ± 4	

the potential region in which the current corresponds essentially to charging of the electrolytic double layer. The considerable hysteresis observed, even at low sweep rates, between the potential at which oxygen is deposited and the potential at which it is removed indicates that these are kinetically slow processes.

(b) Charging curves were obtained in 0.1 N H_2SO_4 and 0.1 N $HClO_4$ with essentially identical results. In Fig. 7 are presented two cathodic charging curves on a Pt electrode in N_2 - saturated, 0.1 N $HClO_4$ and at a constant C. D. of 60 μ A/cm^2 . The potential was forced from the oxygen evolution value to that for hydrogen evolution. Curve I refers to a solution with no added H_2O_2 and Curve II to 10^{-4} M H_2O_2 . The reduction plateaus start at 0.8 V in both I and II. The charge associated with these plateaus is much larger than that expected for a monolayer of oxide ($\sim$ 0.5 milliCoulomb/cm^2 for Pt $(OH)_2$). Thus, molecular oxygen developed during the anodic process must be reduced in addition to the reduction of the surface oxide. The large charge associated with Curve II is probably due to the simultaneous reduction of H_2O_2($H_2O_2 + 2H^+ + 2_e = 2H_2O$, $E^o = 1.77$ V).

(c) Potential decay curves in O_2-saturated solutions exhibited a curious phenomenon. Anodically polarized electrodes decayed upon interruption of the current to potentials more negative (cathodic) than those obtained upon interrupting the current through electrodes which were being polarized cathodically. It was likely that this unexpected behavior was due to the production or decomposition of a soluble product during anodic or cathodic polarization in O_2 - saturated solutions, most probably to the production of H_2O_2 . Therefore, decay curves in N_2 - saturated solutions with and without H_2O_2 were obtained for comparison. In Fig. 8 are presented potential decay curves on interruption of cathodic and of anodic currents (60 μ A/cm^2) in N_2 - saturated 0.1 N $HClO_4$ solutions. The decay of both anodic (Curve I) and cathodic potentials (Curve II) is slow in the absence of O_2 and of H_2O_2 . The potentials approach the same

eventual rest potential ($\sim$ 0.9 V) in about 3 hrs. During this time, the potential of previously anodized specimens is more positive than that of cathodized specimens. However, in the presence of 10^{-4} M H_2O_2 decay is fast (Curve III, A and B) and the rest potential approached from cathodic polarization (0.93 V) is 80 mv more anodic than that approached from anodic polarization (0.85 V). This behavior in solutions containing traces of H_2O_2 is unexpected and is in this sense anomalous. A mechanism for the decay process which leads to different rest potentials is offered in the discussion. Given sufficient time, the rest potential from both sides approaches a common value somewhere in between these two potentials. Essentially identical results were obtained in 0.1 N H_2SO_4.

4. The Resting Potential in H_2O_2 Solutions

The resting potential of Pt electrodes was examined as a function of H_2O_2 concentration (10^{o}, 10^{-1}, 10^{-2}, 10^{-3}, 10^{-4}, and 10^{-5} M) in N_2 - saturated H_2SO_4 solutions (0.1, 1.0, and 5 N). Five identical electrodes were used for each solution composition. The resting potentials in dilute acid solutions (0.1 and 1.0 N H_2SO_4) had a slight tendency of being more anodic with an increase of H_2O_2 concentration. This trend was absent in 5 N H_2SO_4 solutions. On the whole, the results show that the resting potential in a given acid solution is essentially independent of the H_2O_2 concentration. (Table V). The mean values of the resting potential vs a standard hydrogen electrode (SHE), are plotted against pH in Fig. 9. The slope $\partial E/\partial$ pH is about - 0.043 V. The present observation regarding the constancy of the resting potential of smooth Pt in H_2SO_4 solutions with large variations of H_2O_2 concentration (10^{o} - 10^{-5} M) is in agreement with that by Bockris and Oldfield[6]. They observed, however, a pH dependence of the resting potential, $\partial E/\partial$ pH = - 0.059 V, which is larger than the one found here.

5. Electrochemical Reactions of H_2O_2 in H_2SO_4 Solutions

The electrochemical oxidation and reduction of H_2O_2 on bright Pt

TABLE V

Resting Potentials in mv vs Standard Hydrogen Electrode
as a Function of H_2O_2 Concentration
at Different pH(*)

pH	H_2O_2 (M/l)				
	10^{-5}	10^{-4}	10^{-3}	10^{-2}	10^{-1}
1.22 (0.1 N H_2SO_4)	730	751	755	772	773
0.4 (1 N H_2SO_4)	785	766	763	788	802
0.16 (5 N H_2SO_4)	-	-	803	791	792

(*) Potentials are mean values obtained with 4 different electrodes at each H_2O_2 concentration.

electrodes was examined in N_2 - saturated solutions of the following composition:

1 N H_2SO_4	10^{-1} , 1.0 M H_2O_2
5 N H_2SO_4	10^{-3} , 10^{-1} , 1.0M H_2O_2
10 N H_2SO_4	10^{-3} , 10^{-1} , 1.0M H_2O_2

The main features of the results are summarized as follows:

1. For a given acid concentration, both the anodic and the cathodic net currents increased with the increase of H_2O_2 concentration. In 10 N H_2SO_4 solution, both the oxidation and the reduction reactions are essentially first order with respect to H_2O_2 (Figs. 10 and 11). For 5 N and 1 N H_2SO_4 solutions, the apparent reaction orders are lower, and are about 0.3 for 5 N and 0.2 for 2N H_2SO_4. The rates of the oxidation and reduction reactions were, however, increased equally on increasing the H_2O_2 concentration, thus giving essentially constant resting potentials at all H_2O_2 concentrations.

2. Hysteresis was observed for both anodic and cathodic applied currents. The reaction rate increased with time at a given potential during oxidation and decreased with time at a given potential during reduction. Hysteresis became less pronounced with increase in the concentrations of both acid and of H_2O_2.

3. The reduction reaction was more polarized than the oxidation reaction for low acid and low H_2O_2 concentrations; this difference disappeared at large acid or H_2O_2 concentrations.

B. THE OXYGEN REACTION ON GOLD

1. Anodic Polarization

Potentiostatic anodic polarization curves in N H_2SO_4 and N $HClO_4$ were obtained in both N_2 - and O_2 - saturated solutions. A

typical anodic curve in O_2 - saturated N $HClO_4$ is shown in Fig. 12. On anodic polarization above the rest potential (ca. 1.0 V), the current increases smoothly with potential at first. This range comes to an end at about 1.35 V at which potential oxygen evolution takes over. Between 1.35 and 1.45 V a Tafel line is obtained with $b \simeq 0.115$ V and $i_o \simeq 10^{-7}$ A/cm^2. At about 1.45 V a new transition occurs, the current remaining constant ($\sim 1.2 \times 10^{-5}$ A/cm^2) up to about 1.75 V. Beyond this potential oxygen evolution continues, but with a lower exchange current. Hysteresis is observed on decreasing the potential, the Tafel line in the region 1.7 to 1.3 V having a slope of 0.125 V and an exchange current of about 10^{-9} A/cm^2. Essentially the same results are obtained in N_2 - saturated solutions, except that the current in the range of 1.0 to 1.35 V is less ($< 1.5 \times 10^{-7}$ A/cm^2).

The Tafel line obtained during the "down" run, i.e. on decreasing the potential from 2.0 V, can be recorded back and forth with good reproducibility provided the potential stays above 1.35 V. If the electrode is left at a potential of 2.0 V for some time and then a Tafel line is recorded, a straight line is obtained with similar slope but with a lower exchange current. For example, after the electrode was polarized at 2.0 V for one hour the exchange current dropped to 10^{-11} A/cm^2, although the slope did not change substantially.

2. The Reduction of Oxygen

Potentiostatic polarization curves in O_2 and N_2 saturated N $HClO_4$ solutions are shown in Fig. 13. In this particular case, a run in the O_2 - saturated solution was followed by a run in a N_2 - saturated solution and then by a repeat run in O_2 - saturated solution. There are two well-defined regions for the reaction, one at potentials above about 0.7 V and the other at potentials below about 0.5 V with a fairly sharp transition between them; the absolute magnitude of the current at a given potential varied from run to run. Frequently, there was hysteresis between "down" and "up" runs as illustrated in Fig. 14. In other cases, the two regions were de-

veloped more clearly and the i - E characteristics approached Tafel lines with slopes about 0.150 V.

Finally, in certain cases the rest potential was about 0.6 V and the upper section of the polarization curve was missing. In these cases, the electrode could be activated by anodic polarization at potentials 1.6 - 2.0 V whereupon the polarization behavior described above was again obtained. However, the current ($\sim 10^{-7}$ A/cm^2) in the upper potential region was essentially the same in O_2 - saturated and in N_2 - saturated solutions (see Fig. 15).

3. Chronopotentiometric Studies

The formation and reduction of oxides or of adsorbed oxygen on Au electrodes was followed by constant current charging curves and by reduction curves obtained with electrodes which had come to a steady state at various anodic potentials.

Charging curves (Fig. 16) in N_2 - saturated $HClO_4$ solutions show that adsorbed oxygen or oxide begins to appear on the surface in substantial quantities at potentials above 1.35 V. Experiments at 30 μ A/cm^2 showed that the potential rises sharply until it reaches 1.35 V, at which point a break in the potential-time curve is observed. After this, the potential rises less steeply and eventually levels off. On reversing the current (30 μ A/cm^2 cathodic), the potential drops steeply to 1.2 V where a well-defined plateau appears. After a time, t_o, which is proportional to the applied current density, the potential falls steeply to the hydrogen evolution region.

If the anodic polarizing current is switched off when the potential is at the oxygen evolution value (1.8 V at 30 μ A/cm^2), the potential decays to 1.26 V and remains at this value for a period of time before decaying further to a lower value (ca. 1.0 V). The longer the time of anodic polarization, the longer is the period of arrest at 1.26 V. If the polarizing current is switched off, or is reversed just before the arrest

point at 1.35 V, the potential decays to lower values (1.0 V and hydrogen evolution potential, respectively) without showing an arrest. Evidently, the arrest at 1.35 V in the anodic curve and that at about 1.2 V in the cathodic curve represent the same process.

Chronopotentiometric studies of electrodes which had reached a steady state at various anodic potentials (Fig. 17) in N_2 - saturated $HClO_4$ (or H_2SO_4) solutions give essentially the same results as the charging experiments. Oxygen is put on the surface in substantial quantities above 1.4V and is reduced at about 1.2 V. Thus, both methods show that the surface is essentially free of adsorbed oxygen or of oxide at potentials 1.2 V or less, i.e. in the region where oxygen reduction proceeds at appreciable rates.

4. Electrochemical Reactions of H_2O_2 on Gold

The rest potential and the anodic and cathodic reactions of hydrogen peroxide on gold electrodes were studied in solutions containing 10^{-3} to 10^{0}M/l of H_2O_2 and 0.1, 1, and 10 equiv/l of H_2SO_4. The results are given in Table VI. A typical set of polarization curves in 0.1 N H_2SO_4 solution is given in Fig. 18.

The rest potential on Au is independent of the H_2O_2 concentration and the electrochemical reaction orders for both the anodic and the cathodic reactions are essentially unity. This dependence of the rate on H_2O_2 concentration explains immediately why the rest potential does not change with the H_2O_2 concentration.

The anodic polarization curves in H_2O_2 solutions show hysteresis. The anodic curve for 10^{-3} M H_2O_2 (Fig. 19) shows a break at about 1.4 V, i.e. above the potential at which oxide forms on Au (see Section 3). On the "down" run (decreasing potentials) the Tafel line shows a break at about the same potential. The rate of anodic oxidation of H_2O_2 on oxide covered gold electrodes is about 25 times slower than on bare (non-oxidized) surfaces.

TABLE VI

Reaction Orders for Oxidation and Reduction of H_2O_2 on Au Electrodes

$[H_2SO_4]$	Constant Potential E (v)	-log $[H_2O_2]$ molarity	-log i (Amp/cm^2)	$\left(\frac{\partial \log i}{\partial \log [H_2O_2]}\right)_E$ (mean)
Anodic Oxidation of H_2O_2				
10^{-1}N	1.0 V	3	5.19	
		1	3.4	1.0
		0	2.12	
10^{0}N	1.1 V	3	4.3	
		1	2.6	1.4
		0	0.46	
10^{1}N	1.2 V	3	5	
		1	2.4	1.2
		0	1.46	
Cathodic Reduction of H_2O_2				
10^{-1}N	0.6 V	3	5.5	
		1	4.2	0.94
		0	2.9	
10^{0}N	0.7 V	3	5.35	
		1	2.82	0.93
		0	2.3	
10^{1}N	0.6 V	3	4.64	
		1	2.7	0.85
		0	2.3	

V. DISCUSSION

The oxygen reaction on Pt and Au may involve a number of intermediates of which only H_2O_2 is actually stable in solution. Other possible intermediates are O_2^- (or HO_2) and OH which can exist only as adsorbed species on the electrode surface. The relevant thermodynamic potentials for the various reactions and some relevant energies and bond distances are given in Tables VII and VIII.

A. THE OXYGEN REACTION ON PLATINUM

1. The Oxygen Evolution Reaction:

It is clear from the potential sweep curve shown in Fig. 6 that an appreciable amount of oxygen is present on the surface of a Pt electrode at potentials above 0.85 V. This result is in essential agreement with reported data on the oxidation of Pt (9-12). Although it is well established that the oxygen evolution reaction on platinum in acid solution is preceded by the formation of a layer of oxygen on the electrode, there is a divergence of opinion regarding the exact nature of this layer. It has been variously described as a monolayer of different stoichiometric oxides of Pt (PtO, PtO_2, etc.) or as a chemisorbed layer of oxygen (9-14). In any case, it is clear from the present study that the oxygen layer or layers on the electrode modify the kinetics of the oxygen evolution reaction.

The Tafel slope, b = 0.086 V, observed for oxygen evolution on an anodized surface is consistent with a rate-determining discharge step (5). The theoretical slope at 25°C is 0.119 V and is fairly close to the observed value. The deviation between the theoretical and observed values may arise from the assumption in the calculation of the theoretical slope that the energy barrier at the electrode/electrolyte interface is symmetrical. It is probable that the potential energy-distance profile is modified by the oxide layer on the electrode surface, with a consequent change of the transfer coefficient from 0.50 (symmetrical barrier) to 0.68 (observed value).

TABLE VII

Energies and Bond Distances for O_2 and H_2O_2 (*)

Species	Energy (kcal/mol)	Bond Distance (Å)
$O_2(^3\Sigma_g^-)$	117	1.21
$O_2(^1\Delta g)$	95	1.22
$O_2(^1\Sigma_g^+)$	80	1.223
O_2^-	84	1.28
H_2O_2	35	1.47

(*) See ref. 7.

TABLE VIII

Thermodynamic Potentials of Intermediate Reactions(*)

Reaction	E^o
$O_2(aq) + e^- \longrightarrow O_2^-(aq)$	$E^o = -0.6$ V
$HO_2(aq) + e \longrightarrow HO_2^-(aq)$	$E^o = -1.5$ V
$OH(aq) + e \longrightarrow OH^-(aq)$	$E^o = 2.0$ V

(*) Afrer M. G. Evans, N. S. Hush, and N. Uri, ref. 8

The Tafel slope remained essentially the same in a series of 7 successive "down" runs on the same electrode, starting in each case at 3.10^{-4} A/cm^2. However, there was a decrease in the over-all activity of the electrode which was reflected in a somewhat higher potential at 3.10^{-4} A/cm^2. The decrease of the electrode activity is probably due to thickening, or aging, of the anodically formed oxide.

Anodic polarization alternate with cathodic polarization at the same C. D. resulted in an exchange current about three orders of magnitude larger than for anodized surfaces and in a Tafel slope which was also higher (compare Tables I and II). During cathodic polarization, the electrode is stripped of its oxide layer. When the anodic current is imposed, the freshly formed oxide is apparently more active than an aged oxide film, and the exchange current is larger. Furthermore, the transfer coefficient is smaller ($\alpha = 0.45$) on a thin oxide layer than on a layer which has grown to its steady-state thickness.

It should be noted that an alternative interpretation of the results is possible. During cathodic polarization H_2O_2 is formed and this could be oxidized according to (15)

$$H_2O_2 \longrightarrow O_2 + 2H^+ + 2e_o^- \qquad E^o = 0.682 \text{ V}$$

Thus, for a given potential, the combined current due to oxidation of H_2O_2 and of H_2O would be higher than for H_2O oxidation alone. Since the electrode at the anodic potential is in a state of complete concentration polarization with respect to H_2O_2, the potential will rise with time to more anodic values as the local concentration of H_2O_2 drops. The contribution to the current from oxidation of peroxide would lead to an apparent increase of the exchange current when the overpotential curve is determined by this technique. However, the assumption that oxidation of H_2O_2 is responsible for the apparent higher electrochemical activity of freshly anodized surfaces does not explain the increase in overpotential with continued anodization described above. In this case, the H_2O_2 con-

centration is entirely negligible and the current corresponds to oxidation of H_2O only.

The anodic polarization experiments showed that the reaction mechanism for oxygen evolution from H_2O involves a rate-determining discharge step, and that the activity of the electrode surface depends on the extent of anodization (oxide formation) of the Pt surface.

2. Cathodic Reduction of Oxygen

The formation of hydrogen peroxide in the electrochemical reduction of oxygen in alkaline solutions is well established (16 - 18). Similar formation of peroxide is also found in acid solutions. Polarographic measurements show two waves for oxygen reduction on Hg and Pt (19). The first one is considered to be due to the reduction of O_2 to H_2O_2, and the second to the reduction of H_2O_2 to H_2O (19). In the present measurements, it was found that H_2O_2 was formed with high current efficiency in 10 N H_2SO_4. Hunger (20) reported almost quantitative conversion of O_2 to H_2O_2 on active carbon electrodes in H_2SO_4 solutions. Therefore, it appears that H_2O_2 is an important, if not a compulsory, intermediate in the electrochemical reduction of O_2.

In general, H_2O_2 in solution may react with free radicals adsorbed on the electrode and initiate chain reactions, such as

$$OH\ (ads) + H_2O_2 \longrightarrow H_2O + HO_2$$
$$HO_2\ (ads) + H_2O_2 \longrightarrow H_2O + OH\ (ads) + O_2$$

in which oxygen is produced. Weiss (21) has shown that at high ratios of H_2O_2 to H_2SO_4, there is almost complete conversion of adsorbed OH, produced by the electrochemical reduction of H_2O_2 according to the reaction

$$H_2O_2 + e_o^- \longrightarrow OH^- + OH\ (ads),$$

to molecular oxygen. Thus, O_2 evolution occurs with high coulombic efficiency (0. 20 moles O_2/Faraday) on cathodic polarization of Pt in acid solutions containing relatively high concentrations of H_2O_2 . The coulombic efficiency for oxygen evolution drops sharply at small H_2O_2 concentrations.

The constant current experiments for oxygen reduction on Pt (Tables III and IV) were carried out under conditions insuring a minimum amount of H_2O_2 in solution. On the other hand, the potentiostatic runs were steady-state measurements in which the H_2O_2 concentration in solution approached a stationary value at each potential. Therefore, these two sets of measurements refer to different conditions and are discussed separately below.

a) Galvanostatic Experiments:

In view of the above observations, it is assumed that H_2O_2 is an intermediate in the reduction of O_2 on Pt in acid solution. However, since its concentration in solution is vanishingly small, all reactions in which H_2O_2 diffusing from solution may participate are assumed to have negligible rates. Plausible reaction schemes with H_2O_2 as an intermediate have been constructed and are presented in Table IX. The detailed kinetics of these reaction schemes have been calculated using the methods of Bockris (22) and the Tafel parameters for each step are also given in Table IX. The following postulates were made in these calculations:

1. The adsorption step for oxygen on the electrode is fast, i. e. , the oxygen coverage on the electrode surface is in equilibrium with the gas phase.

2. The coverage by molecular oxygen is independent of the potential ($\Delta\phi$).

3. There is no change in the surface properties of the electrode.

4. The reactions are strictly consecutive and one step is rate-determining.

TABLE IX

Reduction of Oxygen $O_2 + 4H^+ + 4e_o^- = 2\,H_2O$ $\quad E^o = 1.23$ V

The Reaction Schemes	$\partial \Delta\phi / \partial \ln i$	
(i)	Low $\Delta\phi$	High $\Delta\phi$
$M - O_2 + H^+ + e_o^- \longrightarrow M - HO_2$	$-RT/\alpha F$	no change
$M - HO_2 + H^+ + e_o^- \longrightarrow M - H_2O_2$	$-RT/(1+\alpha)F$	$-RT/\alpha F$
$M - H_2O_2 + H^+ + e_o^- \longrightarrow M - HO + H_2O$	$-RT/(2+\alpha)F$	$-RT/\alpha F$
$M - HO + H^+ + e_o^- \longrightarrow M + H_2O$	$-RT/(3+\alpha)F$	$-RT/\alpha F$
(ii)		
$M - O_2 + e_o^- \longrightarrow M - O_2^-$	$-RT/\alpha F$	no change
$M - O_2^- + H^+ \longrightarrow M - HO_2$	$-RT/F$	no change
$M - HO_2 + e_o^- \longrightarrow M - HO_2^-$	$-RT/(1+\alpha)F$	$-RT/\alpha F$
$M - HO_2^- + H^+ \longrightarrow M - H_2O_2$	$-RT/2F$	$-RT/\alpha F$
$M - H_2O_2 + e_o^- \longrightarrow OH^- + M - OH$	$-RT/(2+\alpha)F$	$-RT/\alpha F$
$M - OH + e_o^- \longrightarrow M + OH^-$	$-RT/(3+\alpha)F$	$-RT/\alpha F$
(iii)		
$M - O_2 + H^+ + e_o^- \longrightarrow M - HO_2$	$-RT/\alpha F$	no change
$M - HO_2 + H^+ + e_o^- \longrightarrow M - H_2O_2$	$-RT/(1+\alpha)F$	$-RT/\alpha F$
$M - H_2O_2 \longrightarrow M - O + H_2O$	$-RT/2F$	limiting current
$M - O + 2H^+ + 2e_o^- \longrightarrow M + H_2O$	$-RT/2(1+\alpha)F$	$-RT/2\alpha F$
(iv)		
$M - O_2 + H^+ + e_o^- \longrightarrow M - HO_2$	$-RT/\alpha F$	no change
$M - HO_2 + H^+ + e_o^- \longrightarrow M - H_2O_2$	$-RT/(1+\alpha)F$	$-RT/\alpha F$
$M - H_2O_2 \longrightarrow M - O + H_2O$	$-RT/2F$	limiting current
$M - O + H^+ + e_o^- \longrightarrow M - OH$	$-RT/(2+\alpha)F$	$-RT/\alpha F$
$M - OH + H^+ + e_o^- \longrightarrow M + H_2O$	$-RT/(3+\alpha)F$	$-RT/\alpha F$

5. The energy barriers are symmetrical and remain so within the entire potential range.

6. The reactions preceding a given rate-determining step are essentially at equilibrium, while the reactions following it are sufficiently fast to be kinetically unimportant.

Galvanostatic measurements were carried out on both "cathodized" and "anodized" surfaces. A "cathodized surface" was obtained by polarization to potentials near hydrogen evolution. An "anodized surface" is one which was subjected to anodic polarization (at potentials of free oxygen evolution) and was covered by an oxide.

The Tafel slope obtained for cathodized surfaces is 0.056 V at low C. D.'s and 0.108 V at high C. D.'s, while the slope on anodized surfaces is 0.037 V. These values correspond, respectively, to RT/ F, 2RT/F, and 2RT/3F, or, assuming $\alpha = 0.5$, to RT/F, RT/α F, and RT/(1 + α)F. An examination of the reaction schemes for O_2 reduction (Table IX) shows the following:

i) The slope RT/F corresponds to only one step, the second step in the reaction path (ii), viz.,

$$M - O_2^- + H^+ \longrightarrow - M - HO_2 \qquad (1)$$

ii) The higher slope RT/α F corresponds to the first discharge step, viz.,

$$M - O_2 + e_o^- \longrightarrow - M - O_2^- \qquad (2)$$

or

$$M - O_2 + H^+ + e_o^- \longrightarrow - M - HO_2 \qquad (2A)$$

of all the reaction paths at potential values for which the postulates are valid. The same slope is obtained for all other one-electron discharge steps at sufficiently high potentials.

iii) The slope of $RT/(1 + \alpha)F$ appears to correspond to one particular step in all the reaction paths, viz.,

$$M - HO_2 + e_o^- \longrightarrow - M - HO_2^- \quad (3)$$

or

$$M - HO_2 + H^+ + e_o^- \longrightarrow - M - H_2O_2 \quad (3A)$$

According to the above, it would appear that step (1) is rate-controlling on a cathodized surface at lower C. D.'s and that at high C. D.'s the mechanism changes to a rate-determining discharge step, while on an anodized surface the rate-determining step appears to be (3) or (3A).

It is difficult to accept step (1) as the rate-determining process since purely ionic reactions are generally rapid. However, the zero point of charge of Pt is 0.27 V (in 0.1 N H_2SO_4 + 1.0 N Na_2SO_4) (23) which is substantially more negative than the potentials at which oxygen reduction takes place. Therefore, the hydrogen ion concentration at the double layer is probably low and the over-all rate of step (1) may be small although the reaction is intrinsically fast. Although this argument lends some plausibility to the conclusion that step (1) is rate-determining on cathodized surfaces and at low C. D.'s, there are other difficulties with the proposed reaction scheme. For example, Kolthoff and Jordan (24) found that the polarographic reduction wave of oxygen on rotated noble metal electrodes (including Pt) was independent of pH. From this they concluded that hydrogen ions are not involved in the potential determining reactions.

An alternative explanation of the RT/F slope, and of the transition to 2RT/F at higher overpotentials, may be offered in terms of a deviation of the transfer coefficient, α, from its usual value of 0.5. O_2^- or HO_2 is a highly unstable species (E^o = - 0.6 V, see Table VIII) and cannot actually exist in aqueous solutions unless it is stabilized by adsorp-

tion on the electrode surface. The minimum energy required for stabilization at the positive potentials where O_2 reduction takes place can be calculated from the electrode potential and the value of E^o given above and is about 30 kcal/mol. In view of the inherent instability of O_2^- (or HO_2), it may be supposed that the potential energy-distance diagram for

$$O_2 + e_o^- \longrightarrow O_2^- \text{(ads)}$$

departs appreciably from the usual, nearly symmetrical potential profiles and may, in fact, approximate the one depicted in Fig. 20. Since the transfer coefficient is given approximately by a ratio involving the tangents of two Morse curves, in the case depicted in Fig. 20, α will approach 1 at low $\Delta\phi$, while at high $\Delta\phi$ it will approach 0.5. Thus, if step (2) is rate-determining on cathodized surfaces, one can account for the two observed slopes, i.e., RT/F and 2RT/F, by taking into account the highly unstable nature of O_2^-.

Finally, an entirely different interpretation of these two slopes may be offered. In the reaction schemes given in Table IX it is assumed that all reactions are consecutive, one-electron steps. In view of the inherent instability of O_2^- (or HO_2), it is not improbable that the first step in the reduction of O_2 is the direct conversion to HO_2^- via a two-electron reaction. Two-electron transfer reactions are in general less likely than single electron transfers, mainly because the probability of an event decreases sharply as the number of participating particles increases. However, provided electron-transfer from the metal is not seriously impeded by an insulating oxide, it may be assumed that electronic motion is sufficiently fast to adjust the electron density to the most stable configuration corresponding to any particular interatomic distance assumed by the two oxygen atoms during reaction. Therefore, a two-electron reaction may occur if the energy for the formation of O_2^- is about the same, or somewhat larger, than the energy barrier for the transition to $O_2^=$. A two-electron reduction step has been suggested for oxygen reduction in alkaline solutions where the main product is H_2O_2 (25). The reaction

$$O_2 + 2e_o^- \longrightarrow O_2^=$$

or

$$O_2 + H^+ + 2e_o^- \longrightarrow HO_2^-$$

would yield a Tafel slope of RT/2 α F or RT/F if $\alpha = 0.5$. The transition to a higher slope of 2RT/F must be attributed in this case to a shift to a rate-determining step involving reduction of HO_2^- or H_2O_2, for example

$$H_2O_2 + e_o^- \longrightarrow OH^- + OH\ (ads)$$

with slope 2RT/F at high $\Delta\phi$.

Although we cannot rule out unequivocally any of the reaction schemes proposed above, it is likely that the second possibility discussed above corresponds to the actual mechanism. Thus the rate-determining step is probably

$$O_2 + e_o^- \longrightarrow O_2^-$$

with $\alpha \sim 1$ at low $\Delta\phi$ and $\alpha \sim 0.5$ at high $\Delta\phi$.

The Tafel slope on anodized surfaces approaches 2RT/3F or RT/(1 + α)F if $\alpha \sim 0.5$. In this case, the electrode is probably covered by a surface oxide or by a layer of adsorbed oxygen atoms. The overpotential at any given current is appreciably greater on anodized than on cathodized surfaces indicating that the surface oxide constitutes a barrier to reaction. Furthermore, the surface oxide may alter the rate-determining step if there is a change in the relative magnitudes of the interaction energies between intermediates and the electrode surface. Although the Tafel slope suggests that the reduction of HO_2 (or O_2^-) may be rate-determining on anodized surfaces (step 3), this is unlikely in view of the instability of this species. It is probable that the oxide film modifies the potential distribution across the interface and leads to apparent Tafel slopes which are less than those corresponding to a symmetrical barrier for the rate-determining step.

b. Potentiostatic Experiments:

The potentiostatic curves for reduction of O_2 yield a Tafel line with a slope of 0.085 V (Fig. 5). The difference between this set of results and the galvanostatic experiments on cathodized surfaces is attributed to the accumulation of H_2O_2 in solution during the potentiostatic run. Tests for H_2O_2 in solution were positive in the latter case and indicated a stationary concentration - under the particular experimental conditions obtaining in these runs - of about 10^{-4}M.

Hydrogen peroxide accumulating in solution may undergo electrochemical reduction (see below) and may also initiate chain reactions with free radicals adsorbed on the electrode. The general reaction scheme modified to include these possibilities is now

$$O_2 + H^+ + e_o^- \longrightarrow HO_2\,(ads) \qquad (a)$$

$$HO_2 + H^+ + e_o^- \longrightarrow H_2O_2\,(ads) \qquad (b)$$

$$\begin{cases} H_2O_2\,(ads) \longrightarrow H_2O_2\,(sln) & (c) \\ H_2O_2 + e_o^- \longrightarrow OH\,(ads) + OH^- \,(\longrightarrow H_2O) & (d) \end{cases}$$

$$OH\,(ads) + e_o^- \longrightarrow OH^- \,(\longrightarrow H_2O) \qquad (e)$$

or

$$\begin{cases} H_2O_2 + M \longrightarrow M - O + H_2O & (f) \\ M - O + 2e_o^- + H^+ \longrightarrow M + OH^- \,(\longrightarrow H_2O) & (g) \end{cases}$$

with the possible additional reactions

$$\begin{cases} OH\,(ads) + H_2O_2 \longrightarrow HO_2 + H_2O & (h) \\ HO_2 + H_2O_2 \longrightarrow H_2O + OH\,(ads) + O_2 & (i) \end{cases}$$

or

$$2M - O \longrightarrow O_2 + 2M \qquad (j)$$

The chain reactions involving H_2O_2 were proposed by Haber and Weiss (26) while the reactions involving M - O are due to Vielstich (27). These reactions account for the evolution of oxygen on cathodic polarization of Pt in solutions containing H_2O_2 .

The accumulation of H_2O_2 in solution suggests that the rate of a reaction in the subset (d - g) is smaller than that of reaction (a) or (b). This may appear at first to be contradictory to the analysis of the galvanostatic experiments offered above and the suggestion that reaction (a) is probably rate-controlling in the galvanostatic runs. However, it should be noted that the galvanostatic results do not refer to the steady-state reduction of oxygen. Consequently, the reaction in which H_2O_2 may undergo do not enter into the kinetics provided H_2O_2 desorbs from the electrode; on the other hand, the potentiostatic experiments approach steady-state conditions in which the concentration of H_2O_2 builds up to a certain stationary value. In the latter case, the over-all reduction process (eventually to H_2O) is important in determining the polarization curve.

The experiments of Weiss (21) show that reactions (h) - (j) are important only when the ratio of $[H_2O_2]$ to $[H_2SO_4]$, here denoted by γ , is relatively high, say $\gamma > 1$. At low γ's, the coulombic efficiency for O_2 evolution on cathodic polarization of Pt drops to very low values ($< 1\%$), suggesting that reactions (h) - (j) proceed at rates which are negligible compared to those for (d) - (e) or (f) - (g). Since the $[H_2O_2]$ / $[H_2SO_4]$ ratio here is about 10^{-3} , we may neglect reactions (h) - (j). Of the remaining reactions, step (e) is expected to be fast because of the instability of the species involved at the potentials of interest (see Table VIII). The corresponding step (g) in the alternative scheme due to Vielstich is probably also fast in acid solutions. Reaction (f) is expected to yield a limiting current within the region where appreciable polarization is observed. However, the limiting current found on Pt is a diffusion-limited current for O_2 and no evidence was obtained suggesting that it is attributable to a potential-independent, activated step. Therefore, it is likely

that the rate limiting reaction in the potentiostatic runs is step (d), i. e. ,

$$H_2O_2 + e_o^- \longrightarrow OH\ (ads) + OH^-$$

followed by the rapid reduction of OH (ads) to OH^- (or H_2O). The Tafel slope suggests that $\alpha \simeq 0.7$, which is not unreasonable in view of the unstable nature of the hydroxyl radical produced in this reaction (see discussion above).

c) The Redox Reactions of H_2O_2 on Pt Electrodes:

The experimental observations and the discussion above indicate the important role played by H_2O_2 in the over-all reduction of O_2 to H_2O. Consequently, the redox reactions of H_2O_2 on Pt were examined in some detail with the results presented in Sections IV (4) and IV (5).

Our observation regarding the constancy of the resting potentials of a smooth Pt electrode in a H_2SO_4 acid solution with large variations of the H_2O_2 concentration, 10^0 - 10^{-5}M, is in agreement with that by Bockris and Oldfield (6). Such a situation is expected to arise when the reaction is a heterogeneous one and the surface is saturated with some adsorbed species. Bockris and Oldfield (6) suggested from energetic considerations that the H_2O_2 molecule splits up to form two adsorbed OH radicals and that the surface is saturated with these adsorbed radicals. This would mean that the reduction of OH radicals to OH^- or H_2O is a slow reaction. Kolthoff and Jordan (24) observed in their polarographic measurements that substances like methanol, ethanol, glycerol, allyl alcohol, allyl acetate, acrylonitrile and styrene, which react very rapidly with OH radicals, did not affect the "exaltation" of the oxygen wave and hence they concluded that the reaction

$$OH + e_o^- \longrightarrow -OH^-$$

is rapid. The alternative possible explanation, i.e., that H_2O_2 is itself strongly adsorbed on the surface and that the step leading to its decomposition is slow, is also not consistent with the experimental observations recorded above, particularly with a reaction order of unity at high acid concentrations.

Bockris and Oldfield (6) found a simple pH dependence of the resting potentials, the slope $\partial E / \partial$ pH being - 0.059 V at 25°C. Our data show a slope of - 0.043 V instead. The data of Bockris and Oldfield (6) appear rather scattered in the pH region studied here. Our results suggest that the resting potential is a mixed potential determined by more than one reaction. The following reactions may be considered:

1. Reduction of H_2O_2 :

$$H_2O_2 + 2H^+ + 2e_o^- \longrightarrow 2H_2O \qquad E_o = 1.77 \text{ volt}$$

2. Oxidation of H_2O_2 :

$$H_2O_2 \longrightarrow O_2 + 2H^+ + 2e_o^- \qquad E_o = 0.682 \text{ volt}$$

3. Oxidation of Pt:

a) $Pt + 2H_2O \longrightarrow Pt(OH)_2 + 2H^+ + 2e_o^- \qquad E_o = 0.98$ volt

b) $Pt(OH)_2 \longrightarrow PtO_2 + 2H^+ + 2e_o^- \qquad E_o = 1.1$ volt

Since the resting potential in a H_2O solution was more cathodic (0.8 volt) than either of the oxide potentials, it seems unlikely that reactions (3) are important. The potential sweep measurements also show that the steady-state coverage by adsorbed oxygen is very small at potentials below 0.8 V. The resting potentials may be interpreted by the following simple model considering only reactions (1) and (2).

H_2O_2 is oxidized at the electrode according to reaction (2) and reduced according to reaction (1). Since the reduction reaction is much more polarized than the oxidation reaction, the resting potential is represented by A in Figure 21. This postulate regarding the relative

speeds of the oxidation and reduction reaction has some experimental support in that the oxidation reaction (Figs. 10, 11) proceeds with a lower overpotential than the reduction reaction.

With the additional assumption that both the oxidation and the reduction reactions become more polarized (difficult) on a cathodized surface than on an anodized surface, the hysteresis effect in the reduction and oxidation of H_2O_2 (Fig. 11) may be interpreted, as well as the change of the resting potential with electrode pretreatment (Fig. 8). Let it be assumed that OA and RA are the polarization curves for an anodized surface and A represents the mixed, resting potential. On cathodization, both reactions will be more polarized. The polarized curves are now OC and RC, and C is the new resting potential which is shifted in the anodic direction. The decrease of anodic overpotential with time is attributed to an increase in the oxidation reaction when the electrode is covered by a superficial oxide. Similarly, in the cathodic region, the cathodic overpotential increases as the reduction reaction becomes slower on a cathodized surface.

A comparison of Figs. 10 and 11 shows that as the acid concentration is increased, the overpotential for the anodic oxidation of H_2O_2 becomes smaller, while the opposite effect is observed for the cathodic reduction. The reduction reaction consumes hydrogen ions, whereas the oxidation reaction produces hydrogen ions. In the acid concentration range considered, the diffuse layer is negligible and hence the hydrogen ion concentration in the double layer is nearly proportional to the bulk hydrogen ion concentration.

B. THE OXYGEN REACTION ON GOLD

1. Surface Oxidation:

The charging curves and the chronopotentiometric experiments show that the amount of oxygen on a gold surface is very small at potentials below 1.25 V. The surface oxide formed at potentials above 1.35 V probably corresponds to Au_2O_3 since the potential arrest on the anodic charging

curves appears at the Au/Au_2O_3 potential (1.365 V, see ref. 28 and 29). The amount of oxide on the surface increases rapidly with potential and is equivalent to about 3 - 4 layers at 1.70 V.

Gold electrodes in N H_2SO_4 were kept at various potentials between 1.3 and 1.7 V for periods of 5 - 60 minutes, and the surface oxide produced at each potential was then reduced galvanostatically. The total charge corresponding to reduction of the surface oxide is shown as a function of the anodic potential of the Au electrode in Fig. 22. These results are substantially in agreement with similar measurements in N $HClO_4$ reported by Laitinen and Chao (30).

These studies show that a gold electrode is essentially free of adsorbed oxygen and of surface oxides at all potentials below 1.2 V, i.e., at potentials where oxygen reduction takes place, but has a surface oxide, whose thickness increases with potential above 1.4 V, i.e., in the region of oxygen evolution.

2. The Oxygen Evolution Reaction:

The resting potential of Au in acid solutions saturated with O_2 is about 1.0 V. Above this potential, the current becomes increasingly anodic and a Tafel section is found between 1.35 - 1.45 V which apparently corresponds to oxygen evolution on an Au surface which has about one monolayer of adsorbed oxygen. At about 1.45 V a new transition occurs, the current remaining constant up to about 1.70 V. The Tafel line observed above this potential corresponds to oxygen evolution on a surface covered by several layers of Au_2O_3. Fig. 12 shows that the exchange current for oxygen evolution decreases by a factor of 10^2 - 10^3 when a surface oxide is formed on the Au electrode.

On decreasing the potential from 2.0 V towards the rest potential, the Tafel line corresponding to oxygen evolution on an oxide surface is obtained down to a potential of 1.3 V. At this stage, there is a large cathodic transient before a steady anodic current is obtained. This behavior clearly indicates that reduction of the oxide formed during anodic polarization is taking place, viz.,

$$Au_2O_3 + 6H^+ + 6e \longrightarrow 2Au + 3H_2O$$

The Tafel line between 1.7 and 2.0 V can be recorded back and forth with good reproducibility. If, however, the electrode is left polarized at a potential of 2.0 V for some time and then a Tafel line is recorded, a straight line is obtained with a similar slope (0.125 V), but with a lower exchange current. For example, in one experiment the exchange current dropped from 10^{-9} to 10^{-11} amp/cm^2 (with essentially the same Tafel slope) after the electrode was polarized at 2.0 V for one hour. Apparently, the oxide formed on the gold surface, its amount and more probably its defect structure has a definite retarding effect on the oxygen evolution reaction.

Barnartt (31) reported an exchange current of the order of 10^{-22} amp/cm^2 for oxygen evolution on gold in sulfuric acid solutions. This extremely low exchange current may be explained by the fact that a relatively heavy oxide coating was first formed at a C. D. near the upper end of the range (at least 40 coulombs/cm^2 passed). Barnartt (31) observed a lower Tafel slope 0.045 V, as against our value of 0.125 V. This may be due to a genuine change in mechanism. It is of interest to note that the oxide layer on gold does not act as a simple resistance layer as indicated by the fact that a straight Tafel line is obtained. Had the oxide layer acted as a simple ohmic resistance, the Tafel line would have a strong positive deviation at higher current densities.

3. Cathodic Reduction of Oxygen:

The general features of the results presented in Figs. 13 - 15 are that a substantial oxygen reduction current is obtained on bright gold cathodes in acid solutions and that the reduction process shows two clearly defined regions -- one at potentials above 0.7 V and the other at potentials below about 0.5 V. Below 0.35 V, the Tafel line shows a positive deviation towards a limiting current of 2×10^{-3} amp/cm^2. This current is sensitive to stirring of the solution and is therefore identified as the oxygen diffusion

current. With reasonable values for the solubility of oxygen, for the diffusion coefficient of oxygen in solution, and for the thickness of the diffusion layer in the stirred solution, the calculated value of the limiting current agrees well with the observed value (ca. 10^{-3} amp/cm^2).

The transition region between the two sections of the Tafel line shows the characteristic of a limiting current. This current is, however, insensitive to stirring of the solution and hence cannot be a limiting current due to the diffusion of any species in solution. It should be pointed out that the upper region of the polarization curve ($E > +0.6$ V) generally corresponds to current densities of 10^{-6} A/cm^2, or less. At these low current densities, it is not unlikely that small traces of impurities - either reducible substances or traces of catalytically active metals - may complicate the experimental results. A check was provided against accidental contamination by reducible impurities by runs in N_2 - saturated solutions. However, no comparable, direct method for detecting or eliminating noble metal impurities, e.g. traces of Pt, was available. Thus, it is possible that part of the current at the high, positive potentials may be due to reduction taking place at catalytically active impurities on the electrode surface. This possibility cannot be excluded on the basis of the present results.

Assuming that the limiting current is due to coverage of the surface by a species which is decomposed by a non-electrochemical step, one may propose the following scheme (27):

$$M \cdot O_2 + H^+ + e \longrightarrow M - O_2H \quad (1)$$

$$M - O_2H + H^+ + e \longrightarrow M - O_2H_2 \quad (2)$$

$$M - O_2H_2 \longrightarrow M - O + H_2O \quad (3)$$

$$M \cdot O + H^+ + e \longrightarrow M - OH \quad (4)$$

$$M - OH + H^+ + e \longrightarrow M + H_2O \quad (5)$$

This mechanism would give a limiting current when the surface coverage of the species $M - O_2H_2$ reaches saturation. As the potential

becomes less positive (or more negative), this mechanism must break down and a new mechanism corresponding to the second or lower section of the Tafel line must come into play. An alternative mechanism in the lower (less positive) potential region is the electrochemical decomposition of M - O_2H_2 (32) according to the scheme.

$$M - O_2H_2 + H^+ + e \xrightarrow{\text{slow}} M - OH + H_2O \qquad (3a)$$

$$M - OH + H^+ + e \xrightarrow{\text{fast}} M + H_2O \qquad (4a)$$

In short, at low overpotentials (near the reversible oxygen electrode potential), mechanism (1-3) is rate-determining. As the overpotential increases, the coverage by M - O_2H_2 increases. When a saturation value is approached, a limiting current is obtained. But as the overpotential increases further, the alternative mechanism (3a) takes over. This reaction, being electrochemical in nature, has a potential dependent rate and a Tafel line is obtained. Eventually, as the current increases with increasing overpotential, the reaction rate is limited by diffusion of O_2 from the bulk of the solution to the electrode surface.

The upper section of the overpotential curve (potentials between 1.0 and 0.7 V) may correspond to a slow step involving reaction (1) or (3) above. If step (3) is rate-determining, the reaction rate is given by

$$i = 2F\, k_3 P_{O_2}\, (1 - \theta)\, a_H + \exp(-2\Delta\phi/RT)$$

where θ is the surface coverage by adsorbed H_2O_2 and k_3 is a reaction-rate constant. This equation was derived on the assumption that steps (1) and (2) are essentially at equilibrium. If the coverage is small, i.e., $\theta \longrightarrow 0$, then the Tafel slope corresponding to the above equation is

$$\frac{\partial \Delta\phi}{\partial \log i} = -\frac{2.30\, RT}{2F} = 0.030 \text{ V at } 25^{\circ}C.$$

The coverage, θ, increases with increase of overpotential (less positive potentials). Therefore, the rate at which the current increases with $\Delta\phi$ should be less, and the Tafel slope greater, than that predicted by the equation above.

The Tafel slope in the upper section of the polarization curve is about 0.15 V and is substantially greater than the slope predicted by assuming that step (1) is much faster than step (3). Therefore, step (1) is probably also slow, as it is on Pt. The net current in this region is about the same on Pt and Au (potentiostatic runs) suggesting that the rate of (1) is not much different on the two metals. If it is assumed that both step (1) and (3) are slow, then the slope at small θ should approach $RT/\alpha F \simeq 0.120$ V and should increase as the limiting current (high θ) is approached. This mechanism gives values of b which approach the observed Tafel slopes.

In the second section of the Tafel line where step (3a) is rate-determining, the current for high overpotentials is given by

$$i = 3Fka_{H^+} \exp(-\Delta\phi F/RT)$$

The Tafel slope is

$$\frac{\partial \Delta\phi}{\partial \log i} = -\frac{2.30\,RT}{\alpha F} = 0.118 \text{ V at } 25^{\circ}C \text{ with } \alpha = 0.5$$

This agrees with the experimentally observed value of about 0.130 V.

The most important aspect of the results on gold is that the rate of formation of hydrogen peroxide in the cathodic reduction of oxygen at a gold electrode is much lower than that at a platinum electrode. The amount of peroxide detected in a solution when gold was used as an electrode was much smaller than with platinum, although the rate of decomposition of peroxide (at the resting potential) is about ten times larger on a platinum electrode than on a gold electrode under identical conditions (see below).

Electrochemical Reactions of H_2O_2 on Gold

The anodic oxidation and the cathodic reduction of hydrogen peroxide on gold electrodes have been examined for the peroxide concentration of 10^{-3}, 10^{-1}, and 1 M in 10 N, 1 N and 0.1 N sulfuric acid solutions.

Current-potential measurements were made for both the anodic and the cathodic sides. The rates of both the anodic and cathodic reactions increase as the concentration of H_2O_2 is increased. The reaction orders with respect to H_2O_2 have been calculated for the anodic as well as for the cathodic reactions (9) with the results presented in Table VI. Both the anodic and the cathodic reactions are of the first order. This immediately explains why the resting potential of a gold electrode immersed in an acid H_2O_2 solution is independent of H_2O_2 concentration. The same explanation may apply for other noble metal electrodes. The kinetic constant for the decomposition of H_2O_2 on gold at the rest potential as calculated from the above data is 7×10^{-9} sec^{-1} per cm^2. The corresponding value for Pt is 5×10^{-8} sec^{-1} cm^2.

The rate of anodic oxidation of H_2O_2 on an oxide covered gold surface is about 25 times slower than on bare gold surfaces. The anodic curve for 10^{-3} M H_2O_2 (Fig. 19) shows a break at 1.4 V, a potential where oxide formation takes place (Au_2O_3). On the down run (descending potentials) the Tafel line shows a break at the same potential and below this potential the oxide is no loner thermodynamically stable and decomposes. This behavior may be compared with that observed in the same potential range during the anodic oxygen evolution in the absence of H_2O_2.

One important consequence of the reaction order of unity is that for the electrochemical reduction of H_2O_2,

$$H_2O_2 \longrightarrow 2OH_{ads} \qquad \text{(fast)}$$

$$OH_{ads} + H^+ + e \longrightarrow H_2O \qquad \text{(slow)}$$

the suggestion (6), based on rest potential measurements alone, that the surface is saturated with adsorbed OH radicals cannot be correct. If the

surface were saturated with adsorbed OH radicals, the reaction order with respect to H_2O_2 would be zero, which is contrary to observation.

Recently Bianchi et al (33) examined the decomposition of hydrogen peroxide in acid solutions on platinum, iridium, palladium and gold surfaces. They concluded that the peroxide decomposition is a chemical process and not an electrochemical process. On the anodic side, the metal undergoes oxide formation and the peroxide reduces the oxide(s) to give the metal.

$$M(O) + H_2O_2 \longrightarrow M + H_2O + O_2$$

A limiting current is obtained when the surface is completely covered with the oxide(s). This explanation implies that the reaction rate is independent of the H_2O_2 concentration in the working range. This is, however, contrary to observation. The reaction order is unity with respect to H_2O_2 in the case of gold and platinum (H_2O_2 : 10^{-3} - 1M). On the cathodic side, Bianchi et al (33), suggested that peroxide decomposition takes place by reaction with atomic hydrogen adsorbed on the electrode surface, i.e.,

$$H_2O_2 + 2H \longrightarrow 2H_2O$$

A substantial cathodic current (10^{-5} amp/cm^2) was obtained on gold at 0.50 V (33). This would imply that hydrogen ions are discharged on gold at 0.50 V at a rate of 10^{-5} A/cm^2. Charging curves obtained here and by other authors indicate that hydrogen adsorption does not take place on gold until the potential is very near the reversible hydrogen electrode potential. Therefore, the suggested reaction is not possible.

Our measurements indicate a direct electrochemical process for the anodic oxidation as well as for the cathodic reduction of hydrogen peroxide in acid solutions. Chain reactions involving free radicals may occur also at high H_2O_2 concentrations, as indicated above.

REFERENCES

1. O. Kubaschewski and B. E. Hopkins "Oxidation of Metals and Alloys", Butterworths, London, 1953.
2. B. M. W. Trapnell "Chemisorption", Butterworths, London, 1955.
3. M. Stern and A. C. Makrides, J. Electrochem. Soc., 107, 782 (1960).
4. W. J. McG. Tegart "The Electrolytic and Chemical Polishing of Metals", Pergamon Press, New York, 2nd Ed., 1959.
5. J. O'M. Bockris and A. K. M. S. Huq, Proc. Roy. Soc.(London), A237, 277 (1956).
6. J. O'M. Bockris and L. F. Oldfield, Trans. Faraday Soc., 51, 249 (1955).
7. A. G. Gaydon "Dissociation Energies", Chapman and Hall, London, 1953; L. Pauling "Nature of Chemical Bond" Cornell Univ. Press, Ithaca, N. Y., 3rd Ed., 1960.
8. M. G. Evans, N. S. Hush, and N. Uri, Quart. Rev., 6, 186 (1952).
9. F. Will and C. A. Knorr, Z. Elektrochem., 64, 258 (1960).
10. M. Becker and M. W. Breiter, Z. Elektrochem., 60, 1080 (1957).
11. H. Laitinen and C. Enke, J. Electrochem. Soc., 107, 773 (1960).
12. W. Böld and M. W. Breiter, Acta Electrochim., 5, 145 (1961).
13. F. F. Anson and J. J. Lingane, J. Am. Chem. Soc., 79, 4901 (1957).
14. M. W. Breiter and J. L. Weininger, J. Electrochem. Soc., 109, 1135 (1962).
15. W. M. Latimer, "Oxidation Potentials", 2nd Ed., Prentice-Hall, Englewood, N. J., p. 43.
16. W. G. Berl, Trans. Electrochem. Soc., 83, 253 (1943).
17. A. N. Frumkin, Akad. Nauk SSSR, 402 (1955).
18. D. J. G. Ives in "Reference Electrodes" Ed. D. J. G. Ives and G. J. Janz, Academic Press, New York, 1961, p. 366.
19. I. M. Kolthoff and J. J. Lingane, "Polarography", Interscience, New York, p. 557.
20. H. H. Hunger, Proceedings of the Panel on Oxygen Electrodes of the Electrochemical Working Group, 28 Sept. 1961, Power Information Center, Univ. of Pennsylvania.

REFERENCES (cont.)

21. J. Weiss, Trans. Faraday Soc., 31, 668, 1547 (1935).
22. J. O'M. Bockris, J. Chem. Phys., 24, 817 (1956).
23. R. Parsons, "Handbook of Electrochemical Constants" Butterworths, London, 1959, p. 76.
24. I. M. Kolthoff and J. Jordan, J. Am. Chem. Soc., 74, 4801 (1952).
25. M. O. Davies, M. Clark, E. Yeager, and N. F. Hovorka, J. Electrochem. Soc., 106, 56 (1959).
26. F. Haber and J. Weiss, Proc. Roy. Soc. (London) A147, N332 (1934).
27. W. Vielstich, Z. Physik. Chem. (Frankfurt) 15, 409 (1958).
28. T. F. Buehrer and W. E. Roseveare, J. Am. Chem. Soc., 49, 1989 (1927).
29. R. H. Gerke and M. D. Rourke, J. Am. Chem. Soc., 49, 1855 (1927).
30. H. A. Laitinen and M. S. Chao, J. Electrochem. Soc., 108, 726 (1961)
31. S. Barnartt, J. Electrochem. Soc., 106, 722 (1959); ibid, 106, 991 (1959).
32. H. Gerischer, Z. Phys. Chem. (N. F.), 6, 178 (1956).
33. G. Bianchi, G. Caprioglio, S. Malaguzzi, F. Mazza, and T. Mussini, AFOSR TN 60-299, May 1960 (Contract No. AF 61(052)-260).

FIGURE CAPTIONS

Figure

1a Electrochemical cell for polarization measurements. Electrodes are mounted so that only Teflon and Pyrex, in addition to the electrode, are exposed to solution.

1b Purification train for gaseous oxygen.

1c Electrical circuit for potential sweep measurements. The working electrode (W) is at ground. The reference (R) and auxiliary (A) electrodes are platinized Pt.

2 Anodic, galvanostatic polarization curves on Pt. Curve I was obtained on decreasing the current density (anodized electrodes); Curve II was obtained by alternate anodic and cathodic polarization in the way described in the text. The solution was 0.1 N H_2SO_4 in both cases.

3 Time-potential curves with Pt for alternate anodic and cathodic polarization in 0.1 N H_2SO_4 .

4 Galvanostatic polarization curves for O_2 reduction on Pt in 0.1 N H_2SO_4 . Curve I was obtained with a cathodically pre-polarized electrode and Curve II with an anodically pre-polarized electrode.

5 Potentiostatic, steady-state polarization curve for oxygen reduction on Pt in N H_2SO_4 .

6 Current-potential curves for Pt in 2N H_2SO_4 obtained at a sweep rate of 3 V/sec. The ionization of adsorbed hydrogen is essentially complete at 0.4 V. Oxygen begins to be adsorbed at 0.85 V on the cathodic sweep, it is removed completely when the potential reaches 0.5 V.

7 Galvanostatic, cathodic charging curves with Pt electrodes in N_2 - saturated, 0.1 N $HClO_4$. I - no H_2O_2 ; II - 10^{-4} M H_2O_2 . In both cases, $i_c = 60\ \mu A/cm^2$.

FIGURE CAPTIONS (cont.)

Figure

8 Anodic and cathodic decay curves with Pt in N_2 - saturated 0.1 N $HClO_4$. I - Anodic decay curve with no H_2O_2 ; II - Cathodic decay with no H_2O_2 ; III - Potential decay after successive polarization at 60 μ A/cm^2 for varying times in a 10^{-4} M H_2O_2 solution. Curve III - A is obtained after cathodic and Curve III-B after anodic polarization.

9 The rest potential of Pt in H_2O_2 solutions as a function of pH. Potentials are against a standard hydrogen electrode and each point is the mean value measured over the range 10^{-5} to 10^{0} M H_2O_2.

10 Polarization curves for anodic oxidation and cathodic reduction of H_2O_2 on Pt in 10 N H_2SO_4. Curve I is for 10^{-3} M H_2O_2 and Curve II for 10^{-1} M H_2O_2.

11 Polarization curves for anodic oxidation and cathodic reduction of H_2O_2 on Pt. The solution compositions were:

	H_2SO_4 (N)	H_2O_2 (M)
a)	1.0	1×10^{-1}
b)	1.0	1.0
c)	5.0	1×10^{-3}
d)	5.0	1×10^{-1}
e)	5.0	1.0
f)	10.0	1×10^{-3}
g)	10.0	1×10^{-1}
h)	10.0	1.0

12 Steady-state, potentiostatic, anodic polarization curves on gold in N $HClO_4$. Open circles are for ascending potentials and full circles for descending potentials.

FIGURE CAPTIONS (cont.)

Figure

13 A potentiostatic, cathodic polarization curve for Au in O_2 - saturated, N H_2SO_4 solution. Open circles are for decreasing potentials and full circles for increasing potentials.

14 A potentiostatic, cathodic polarization curve for Au in O_2 - saturated, N H_2SO_4 solution. The squares indicate the polarization curve obtained on the same electrode in a N_2 - saturated solution.

15 A potentiostatic, cathodic polarization curve for Au in N_2 - and O_2 - saturated, N H_2SO_4 solutions.

16 Galvanostatic (30 μ A/cm^2) curves on Au in N_2 - saturated, N H_2SO_4 solution.

17 Galvanostatic (15.1 μ A/cm^2), cathodic discharge curves on an Au electrode previously held potentiostatically at a series of increasing potentials (0.9 to 1.5 V).

18 Polarization curves for H_2O_2 on Au electrodes in N_2 - saturated, 0.1 N H_2SO_4.

19 Potentiostatic, polarization curves for the oxidation of H_2O_2 on oxide-covered (full circles) and oxide-free (open circles) Au electrodes. Solutions were 10^{-3} M H_2O_2 and 0.1 N H_2SO_4.

20 Schematic potential energy-distance diagram for the reduction of O_2 to O_2^-.

21 Schematic, current-potential diagram for the H_2O_2 couple on Pt electrodes.

22 The extent of surface coverage by oxygen as a function of potential; 300 μ coul/cm^2 correspond approximately to a monolayer of oxygen.

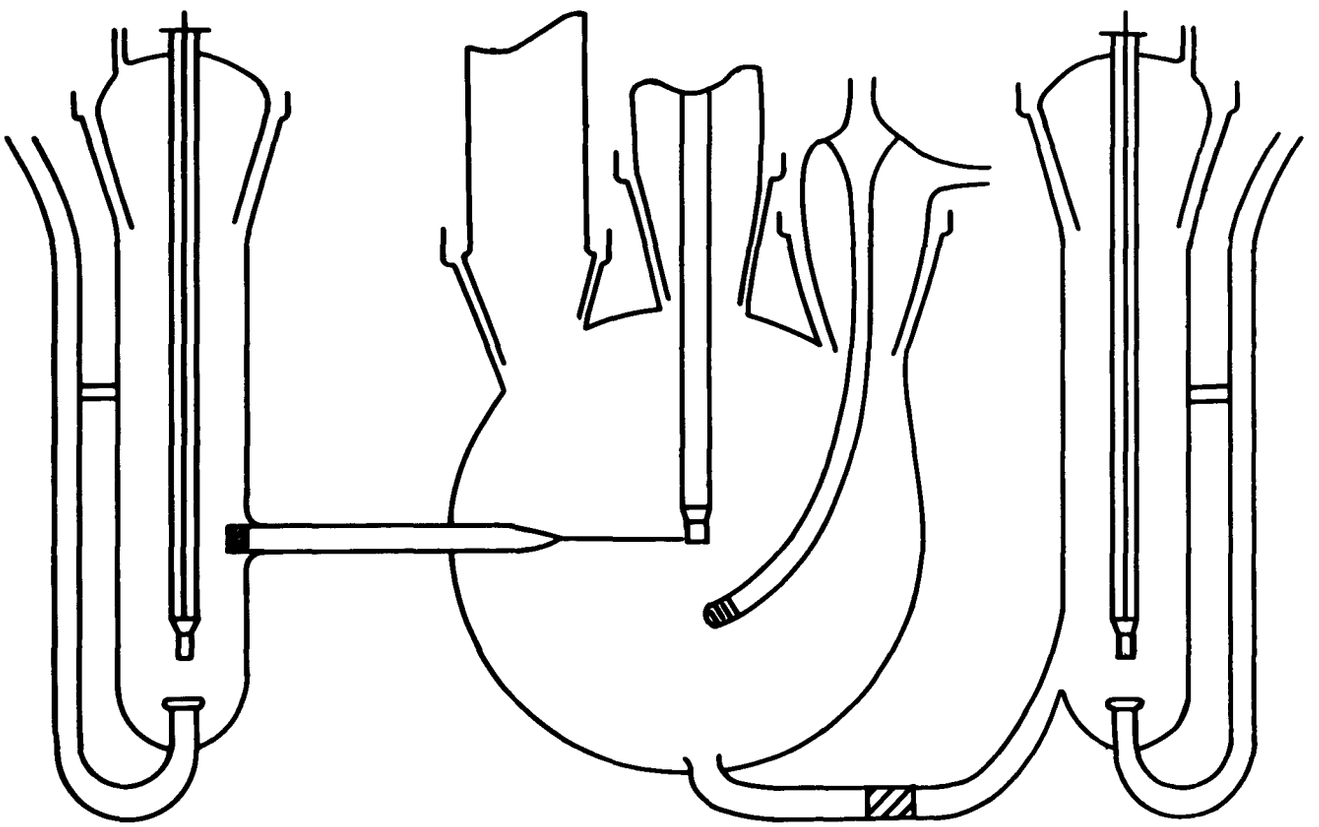

FIG. 1 a

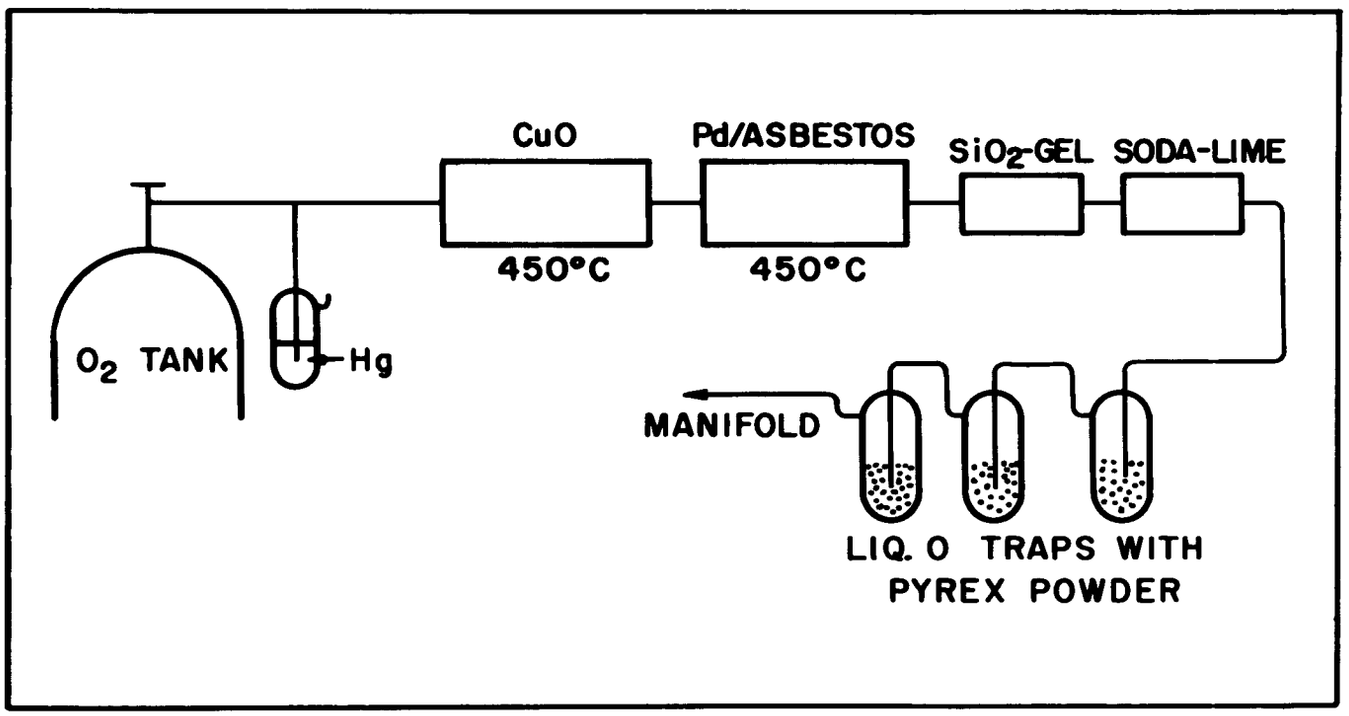

OXYGEN PURIFICATION TRAIN

FIG. 1 b

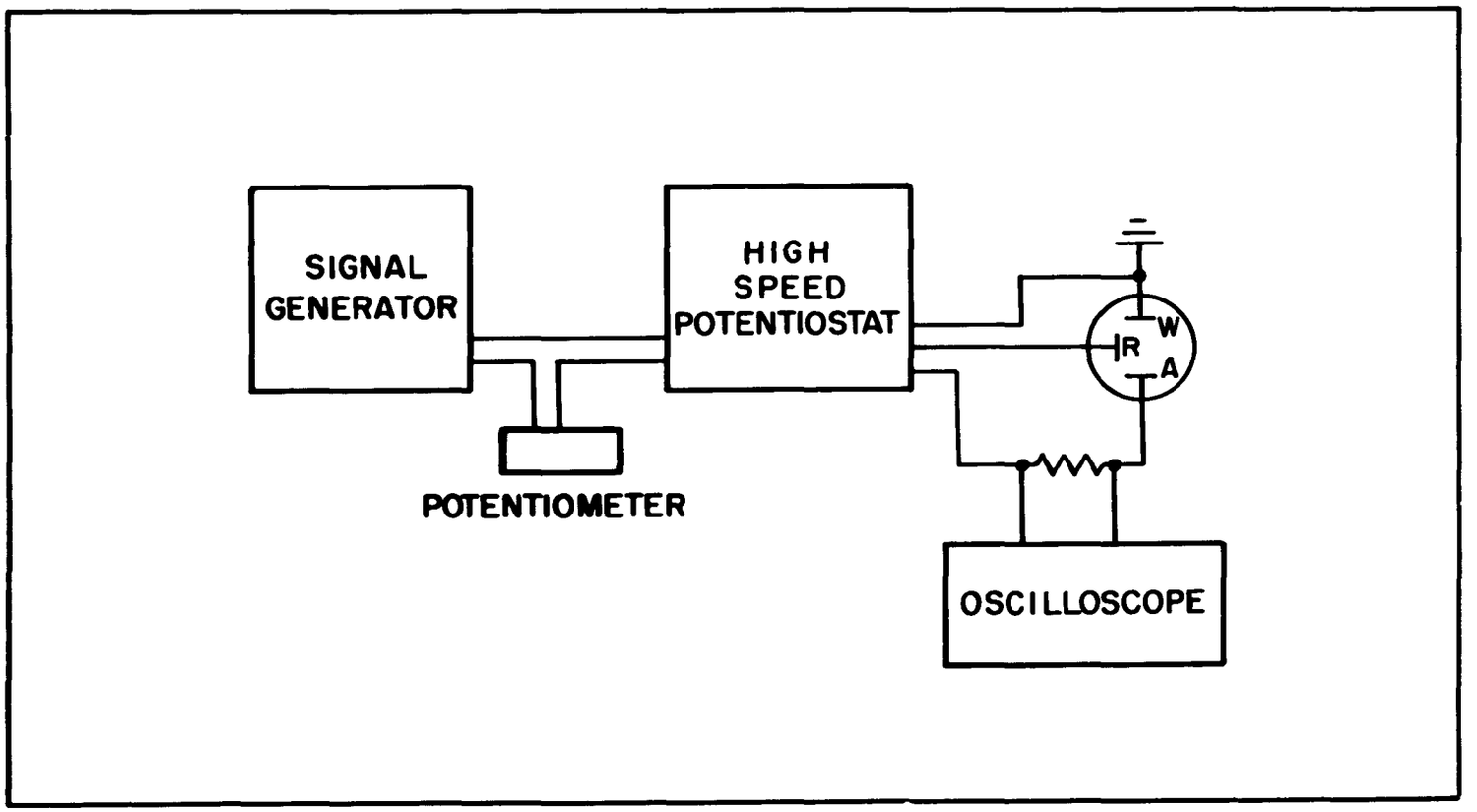

CIRCUIT FOR POTENTIAL SWEEP MEASUREMENTS

FIG. 1 c

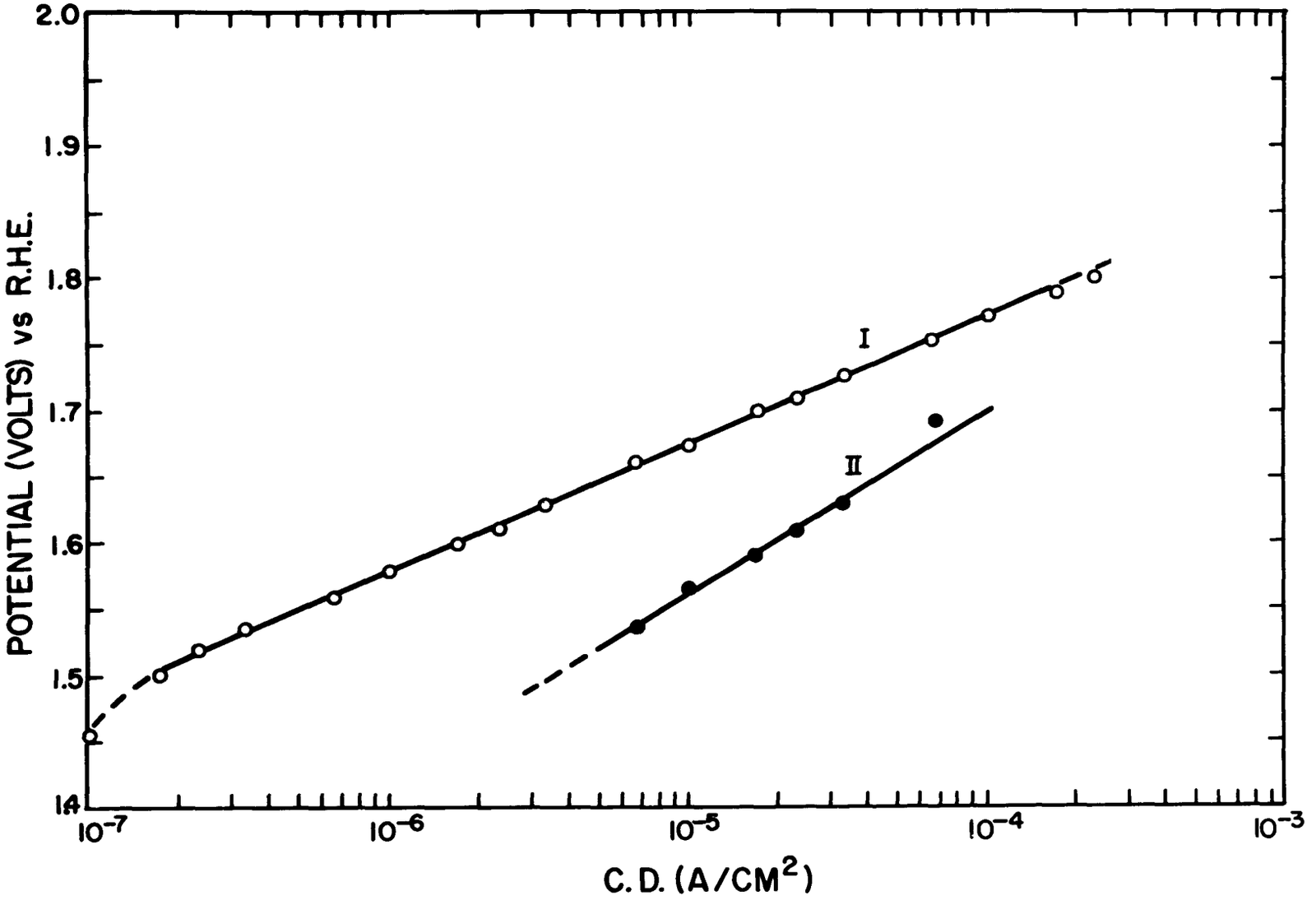
2.0
1.9
1.8
1.7
1.6
1.5
1.4
POTENTIAL (VOLTS) vs R.H.E.
I
II
10^{-7}
10^{-6}
10^{-5}
10^{-4}
10^{-3}
C.D. (A/CM^2)

FIG. 2

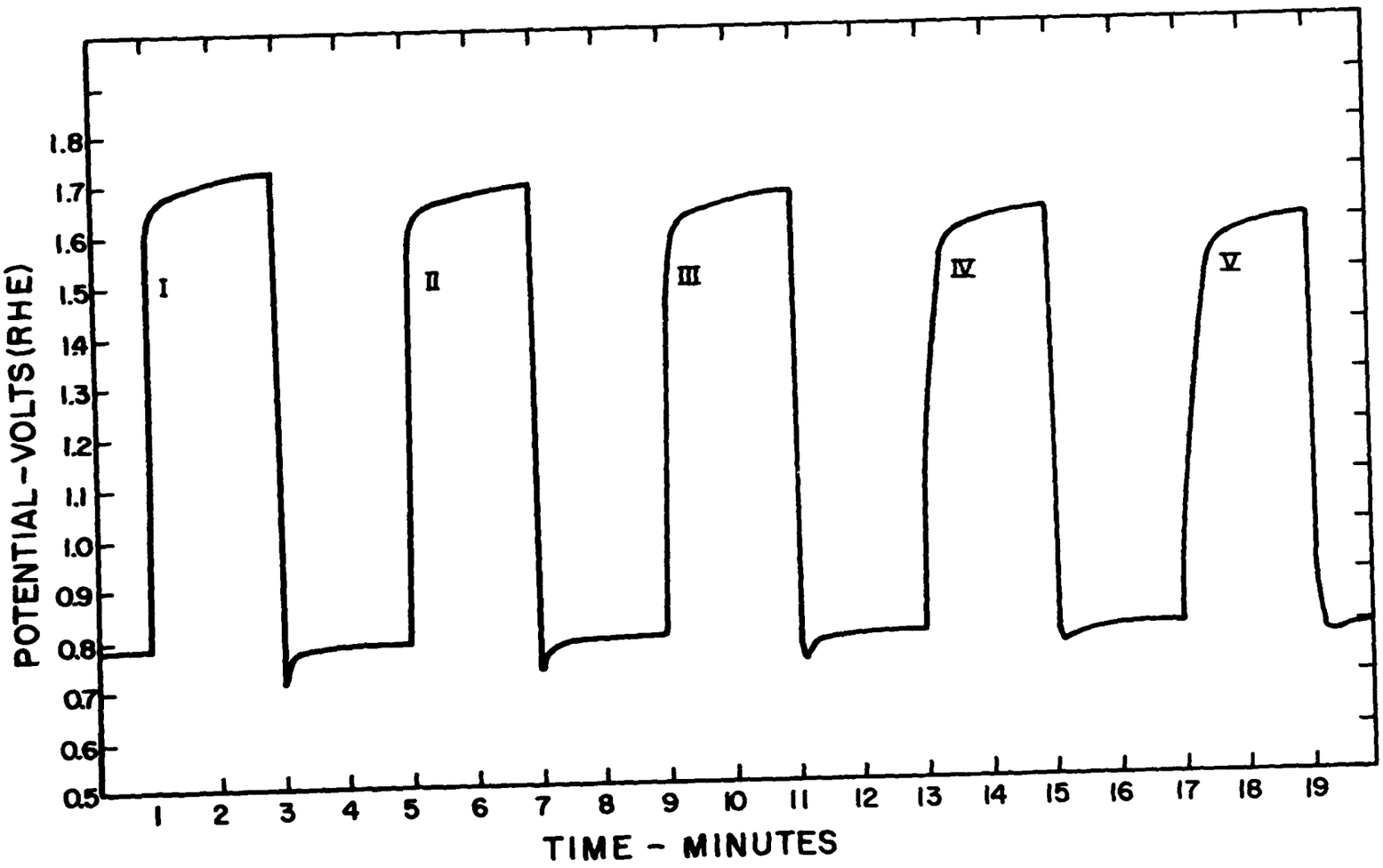
POTENTIAL - VOLTS (RHE)
1.8
1.7
1.6
1.5
1.4
1.3
1.2
1.1
1.0
0.9
0.8
0.7
0.6
0.5
I
II
III
IV
V
1 2 3 4 5 6 7 8 9 10 11 12 13 14 15 16 17 18 19
TIME - MINUTES

FIG. 3

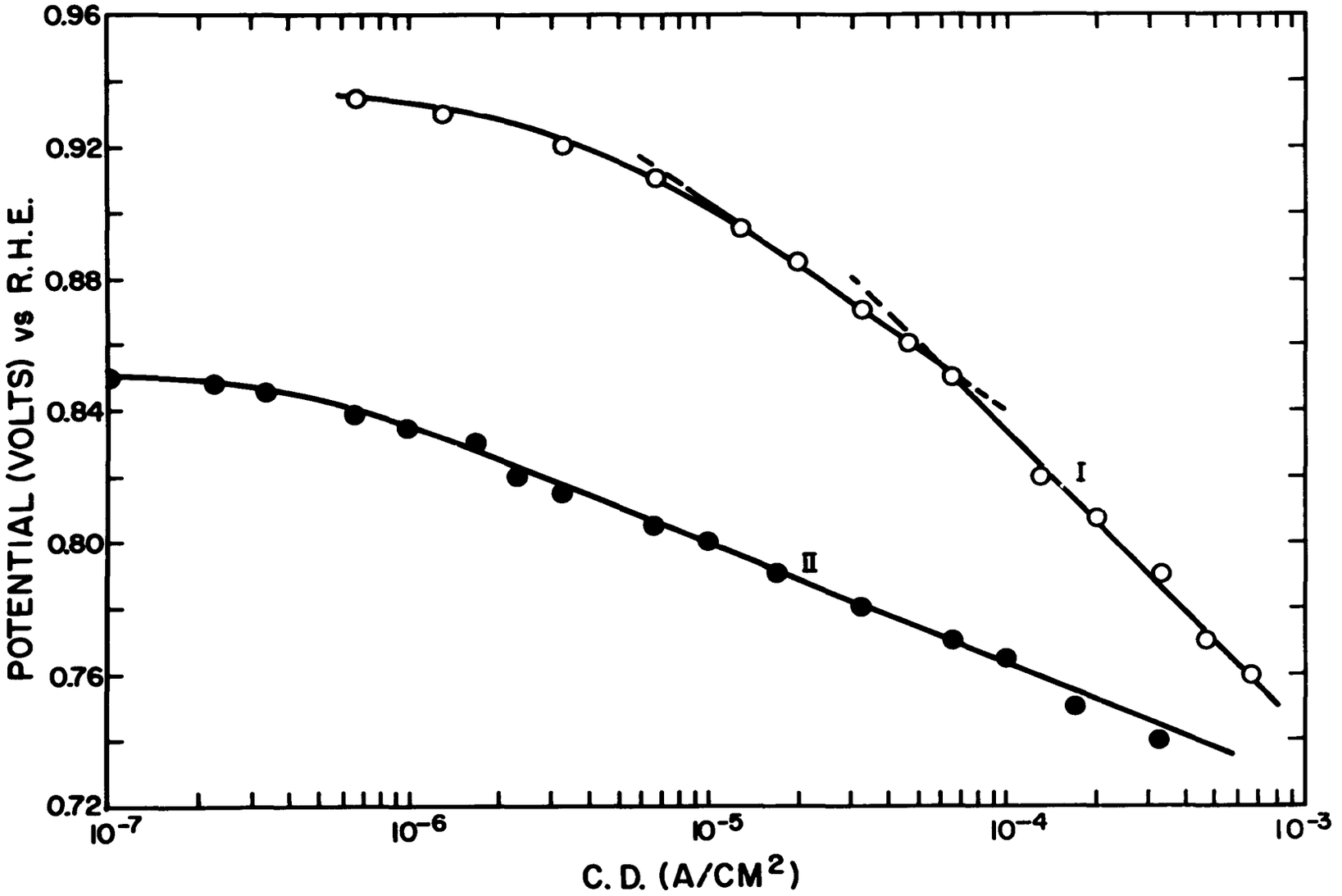
0.96
0.92
0.88
0.84
0.80
0.76
0.72
POTENTIAL (VOLTS) vs R.H.E.
10-7
10-6
10-5
10-4
10-3
C. D. (A/CM2)
I
II

FIG. 4

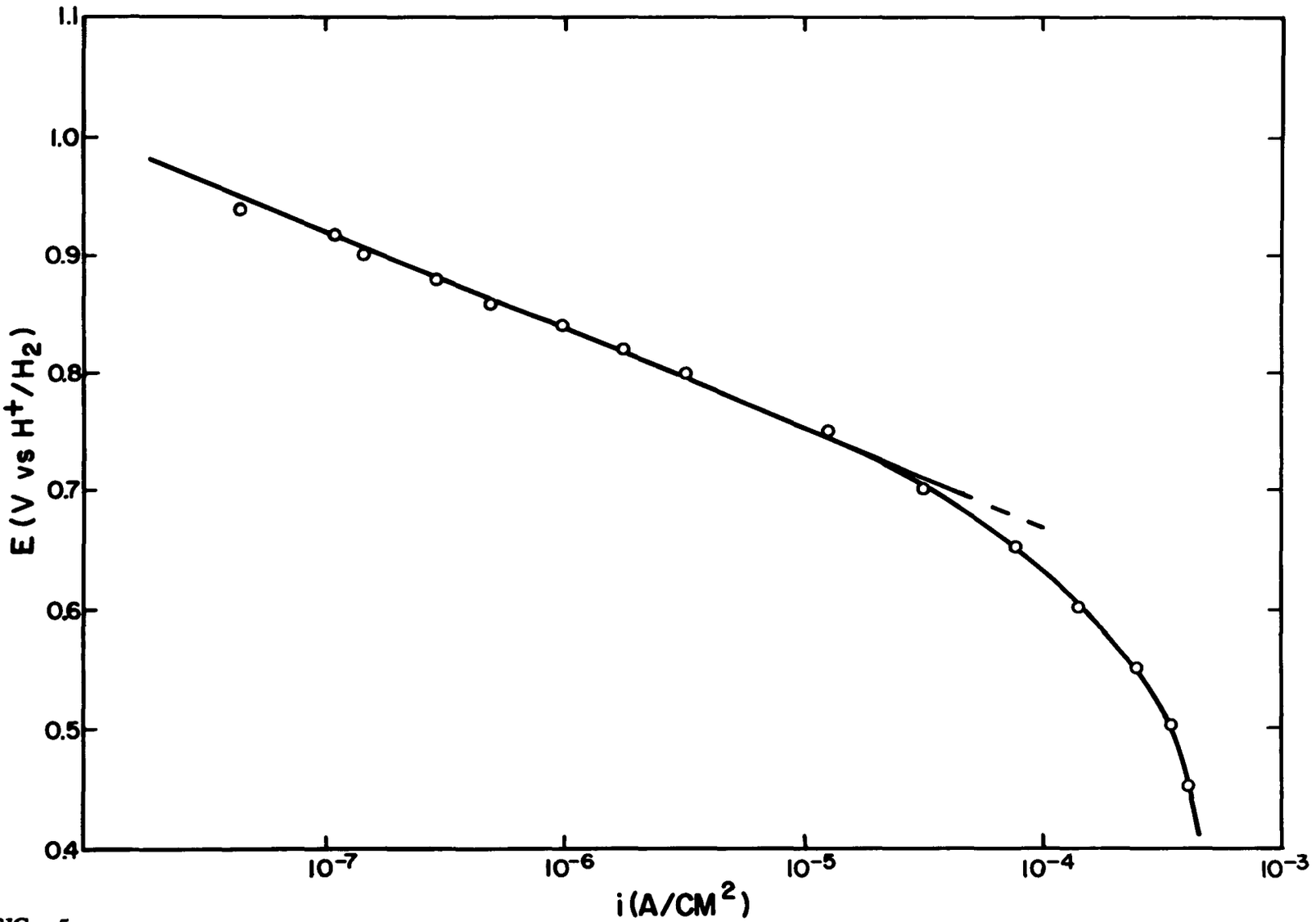

FIG. 5

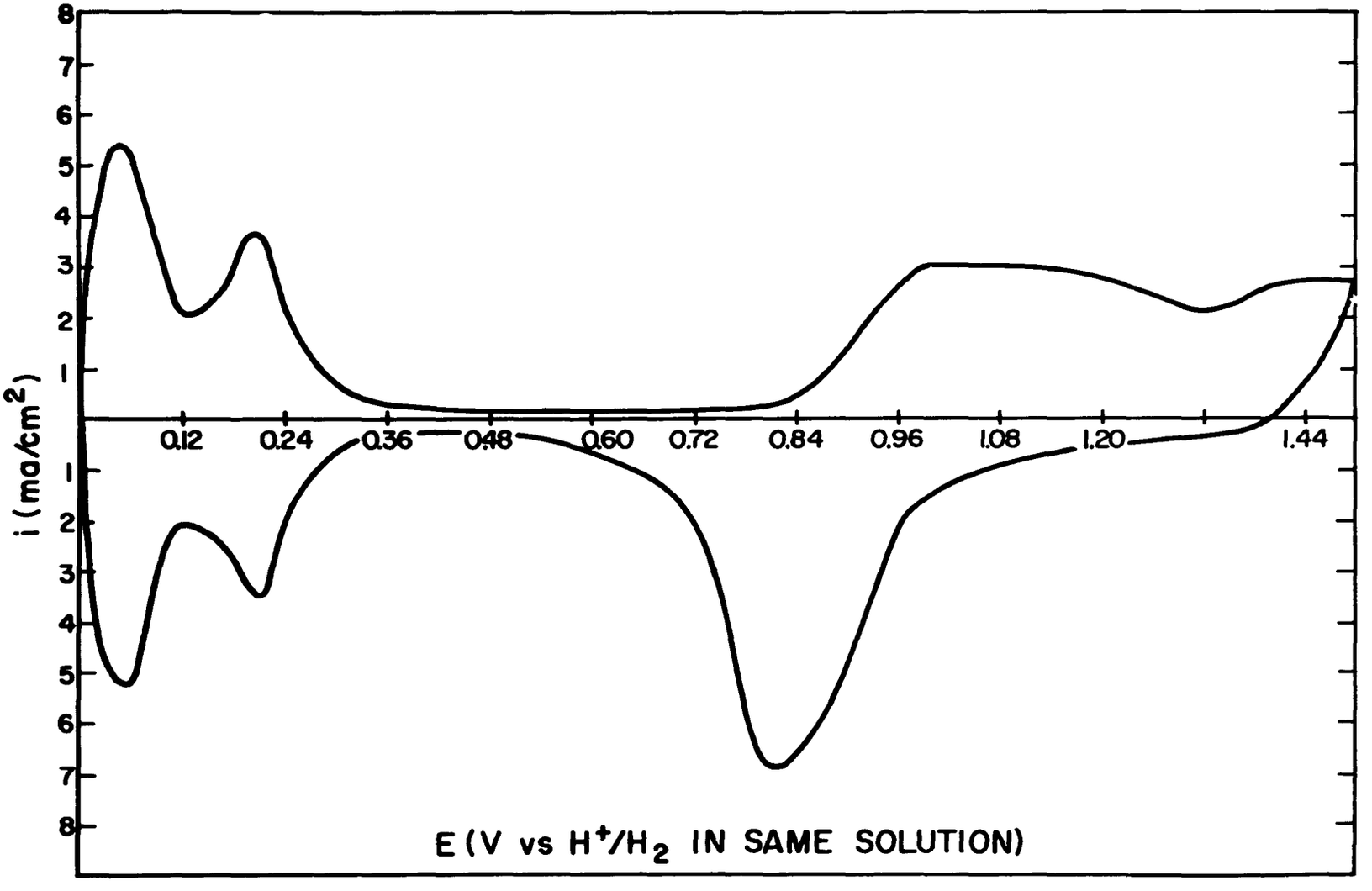
8
7
6
5
4
3
2
1
0.12
0.24
0.36
0.48
0.60
0.72
0.84
0.96
1.08
1.20
1.44
i (ma/cm²)
E (V vs H⁺/H₂ IN SAME SOLUTION)

FIG. 6

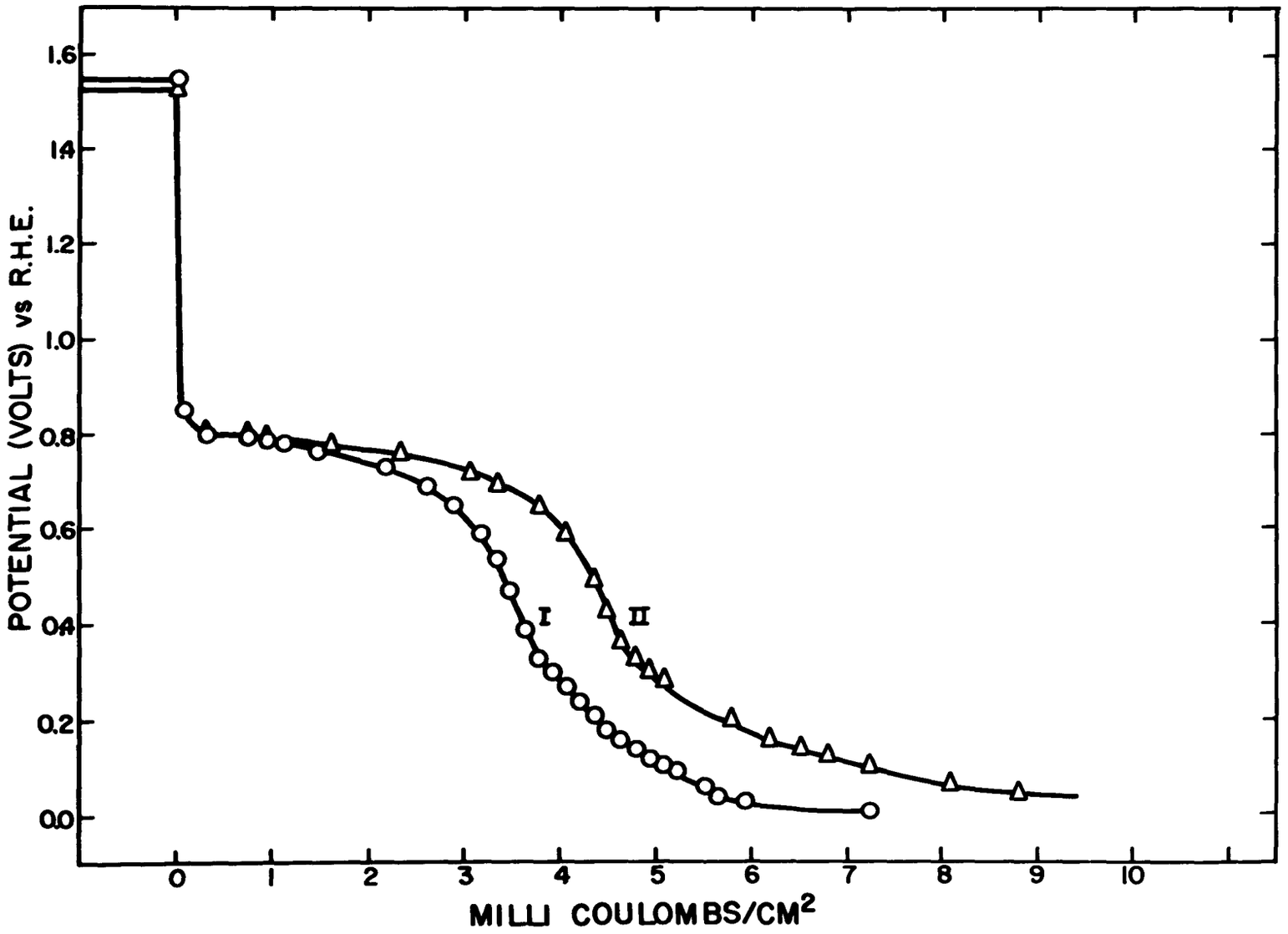
POTENTIAL (VOLTS) vs R.H.E.
1.6
1.4
1.2
1.0
0.8
0.6
0.4
0.2
0.0
0
1
2
3
4
5
6
7
8
9
10
MILLI COULOMBS/CM2
I
II

FIG. 7

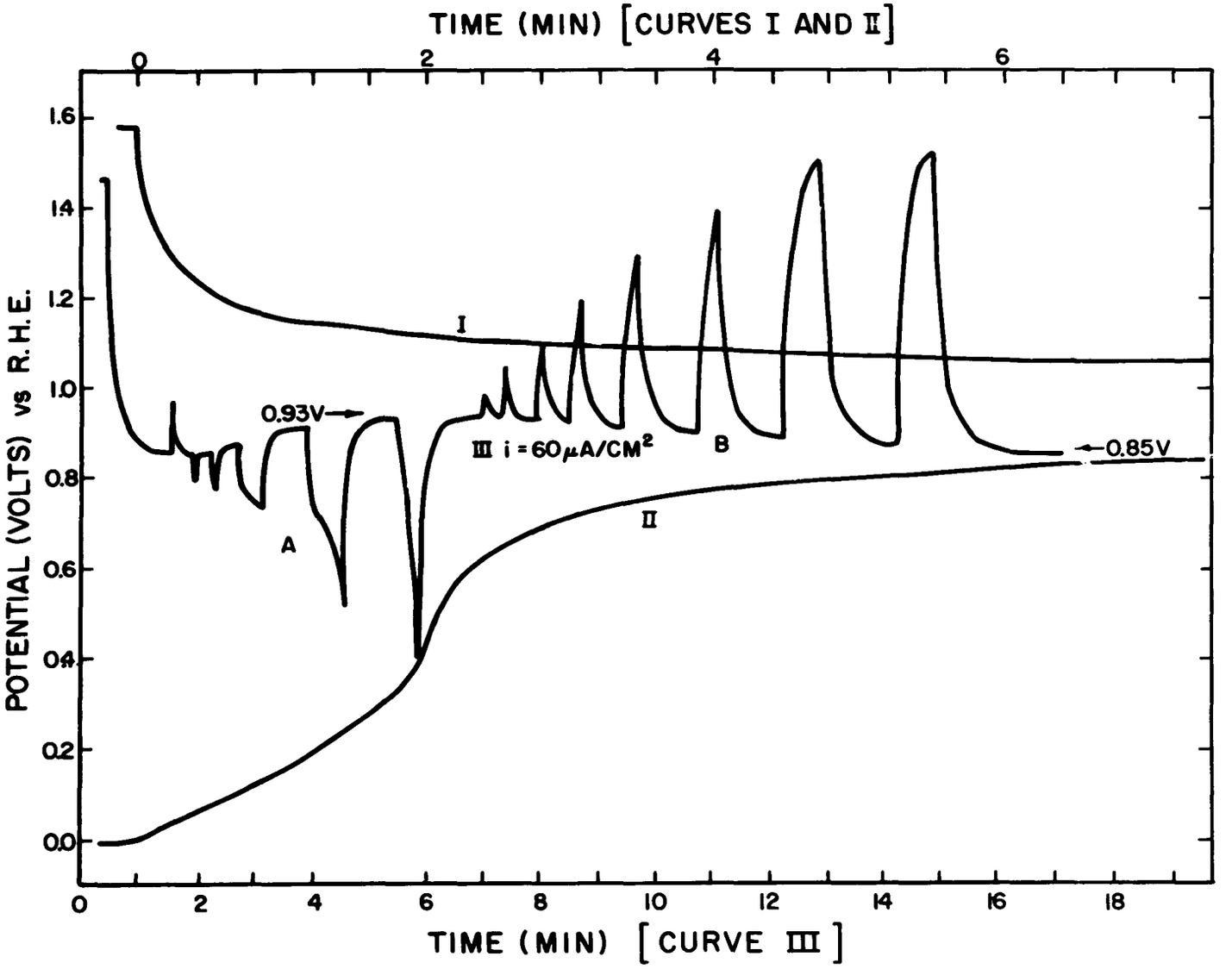
TIME (MIN) [CURVES I AND II]
0
2
4
6
1.6
1.4
1.2
1.0
0.8
0.6
0.4
0.2
0.0
POTENTIAL (VOLTS) vs R.H.E.
I
II
III i = 60μA/CM²
0.93V
0.85V
A
B
0
2
4
6
8
10
12
14
16
18
TIME (MIN) [CURVE III]

FIG. 8

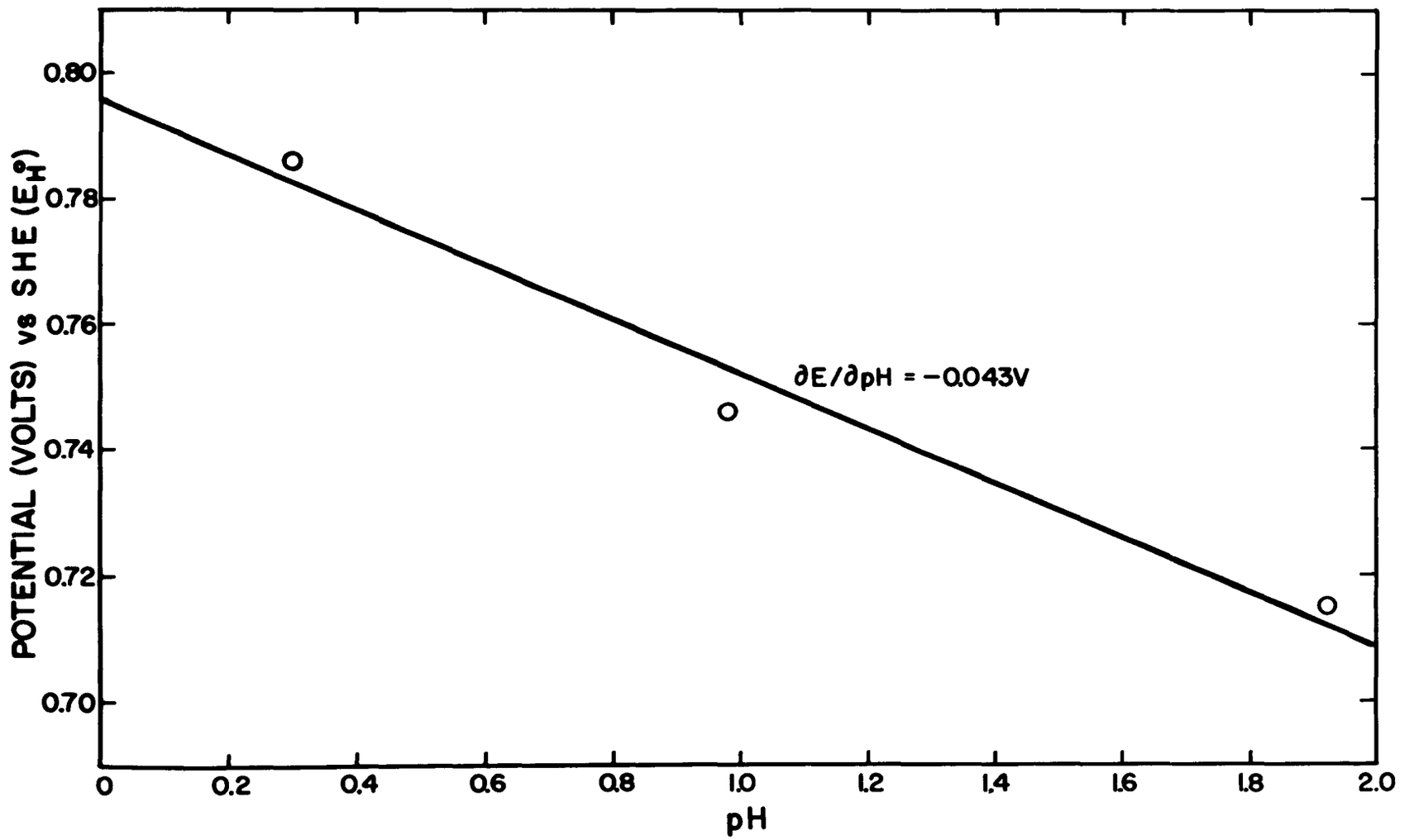
POTENTIAL (VOLTS) vs SHE (E_H°)
0.80
0.78
0.76
0.74
0.72
0.70
$\partial E/\partial pH = -0.043V$
0
0.2
0.4
0.6
0.8
1.0
1.2
1.4
1.6
1.8
2.0
pH

FIG. 9

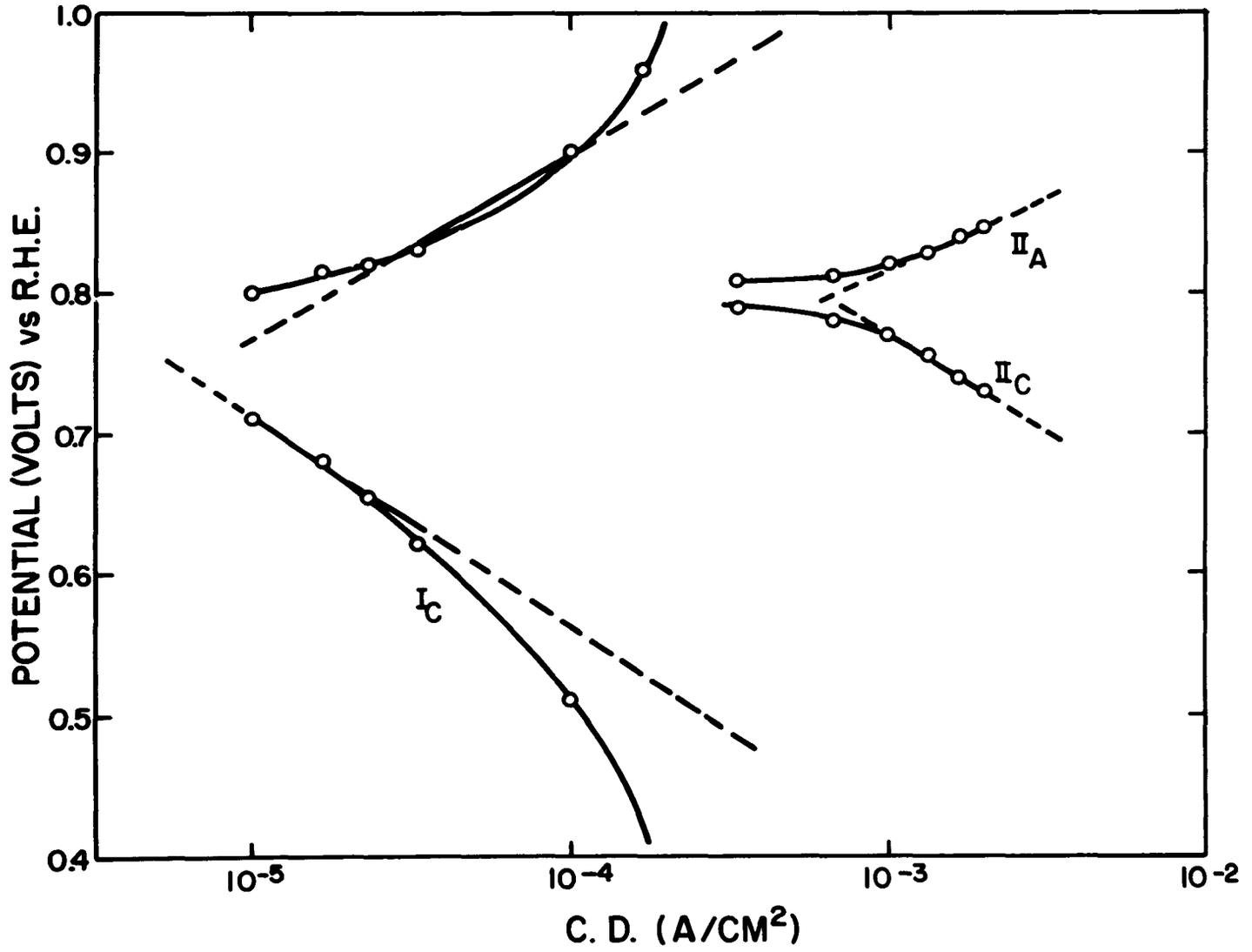
1.0
0.9
0.8
0.7
0.6
0.5
0.4
POTENTIAL (VOLTS) vs R.H.E.
10^{-5}
10^{-4}
10^{-3}
10^{-2}
C. D. (A/CM^2)
I_C
II_A
II_C

FIG. 10

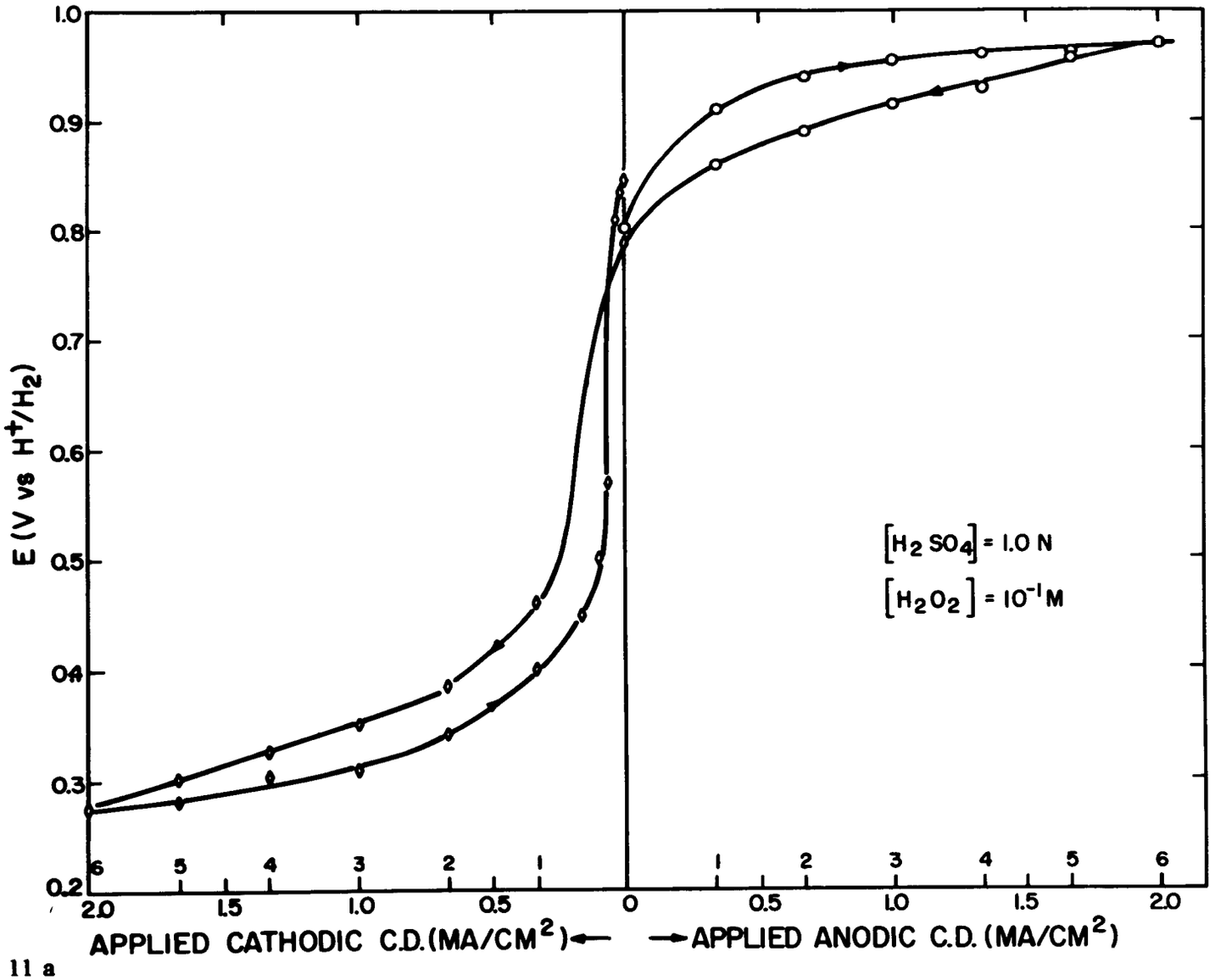
E (V vs H+/H2)
1.0
0.9
0.8
0.7
0.6
0.5
0.4
0.3
0.2
[H2 SO4] = 1.0 N
[H2O2] = 10-1M
6 5 4 3 2 1
2.0 1.5 1.0 0.5 0
1 2 3 4 5 6
0.5 1.0 1.5 2.0
APPLIED CATHODIC C.D.(MA/CM2)←
→APPLIED ANODIC C.D. (MA/CM2)

FIG. 11 a

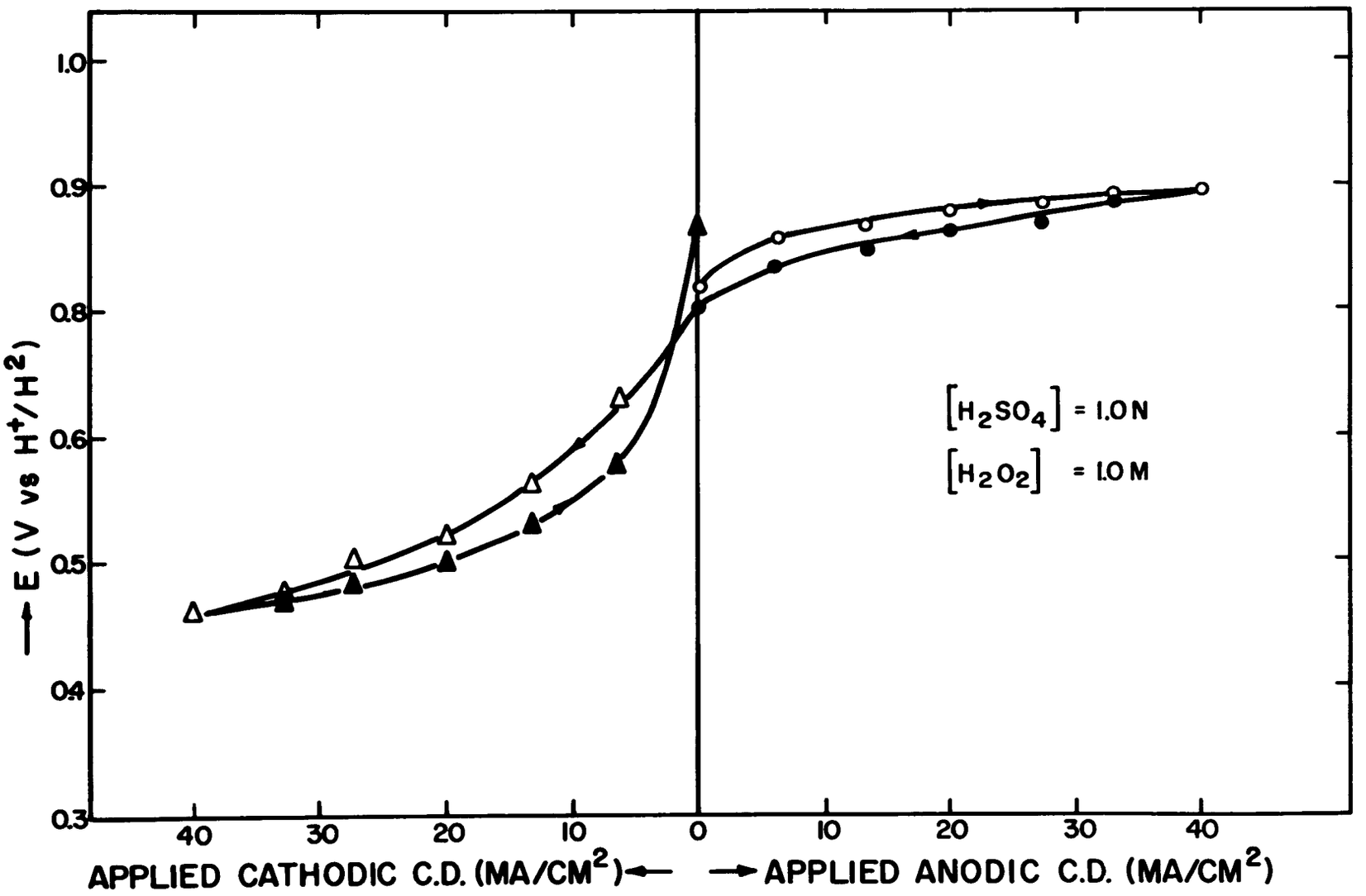
1.0
0.9
0.8
0.6
0.5
0.4
0.3
E (V vs H+/H2)
40
30
20
10
0
10
20
30
40
APPLIED CATHODIC C.D. (MA/CM2)
APPLIED ANODIC C.D. (MA/CM2)
[H2SO4] = 1.0 N
[H2O2] = 1.0 M

FIG. 11 b

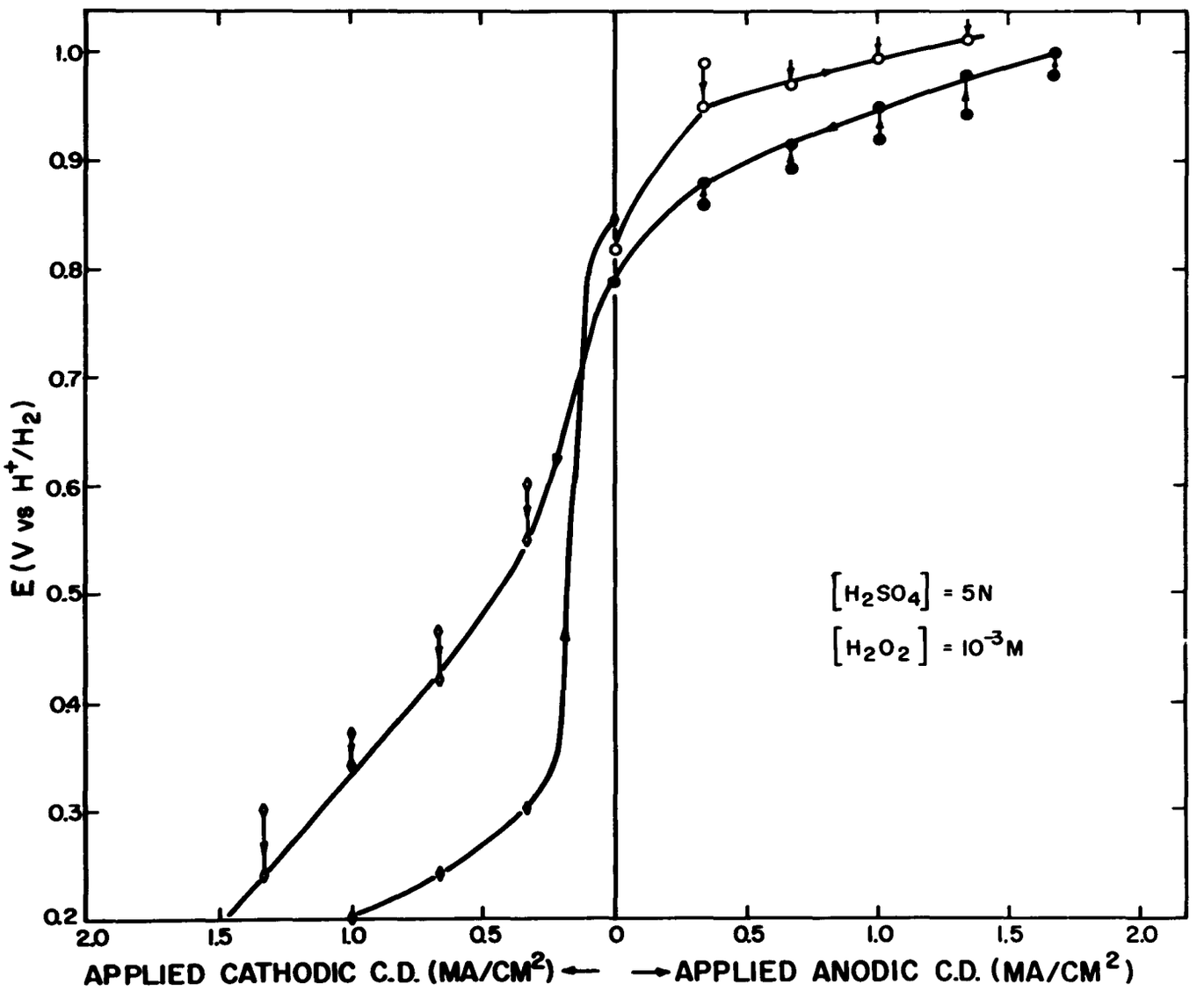
1.0
0.9
0.8
0.7
0.6
0.5
0.4
0.3
0.2
E (V vs H+/H2)
2.0
1.5
1.0
0.5
0
0.5
1.0
1.5
2.0
APPLIED CATHODIC C.D. (MA/CM2) ←
→ APPLIED ANODIC C.D. (MA/CM2)
[H2SO4] = 5N
[H2O2] = 10-3M

FIG. 11 c

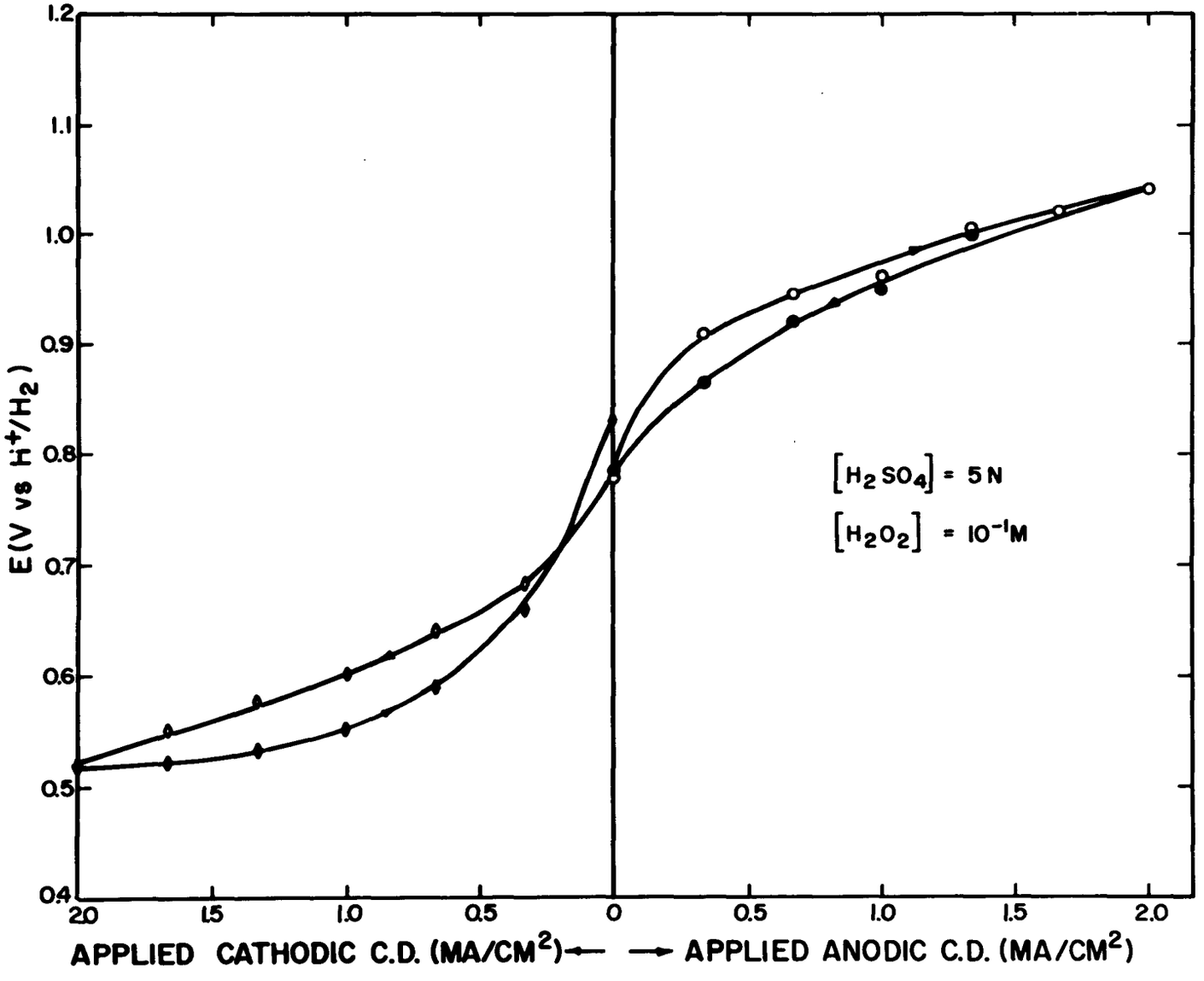
1.2
1.1
1.0
0.9
0.8
0.7
0.6
0.5
0.4
E(V vs H+/H2)
[H2SO4] = 5N
[H2O2] = 10-1M
2.0
1.5
1.0
0.5
0
0.5
1.0
1.5
2.0
APPLIED CATHODIC C.D. (MA/CM2)
APPLIED ANODIC C.D. (MA/CM2)

FIG. 11 d

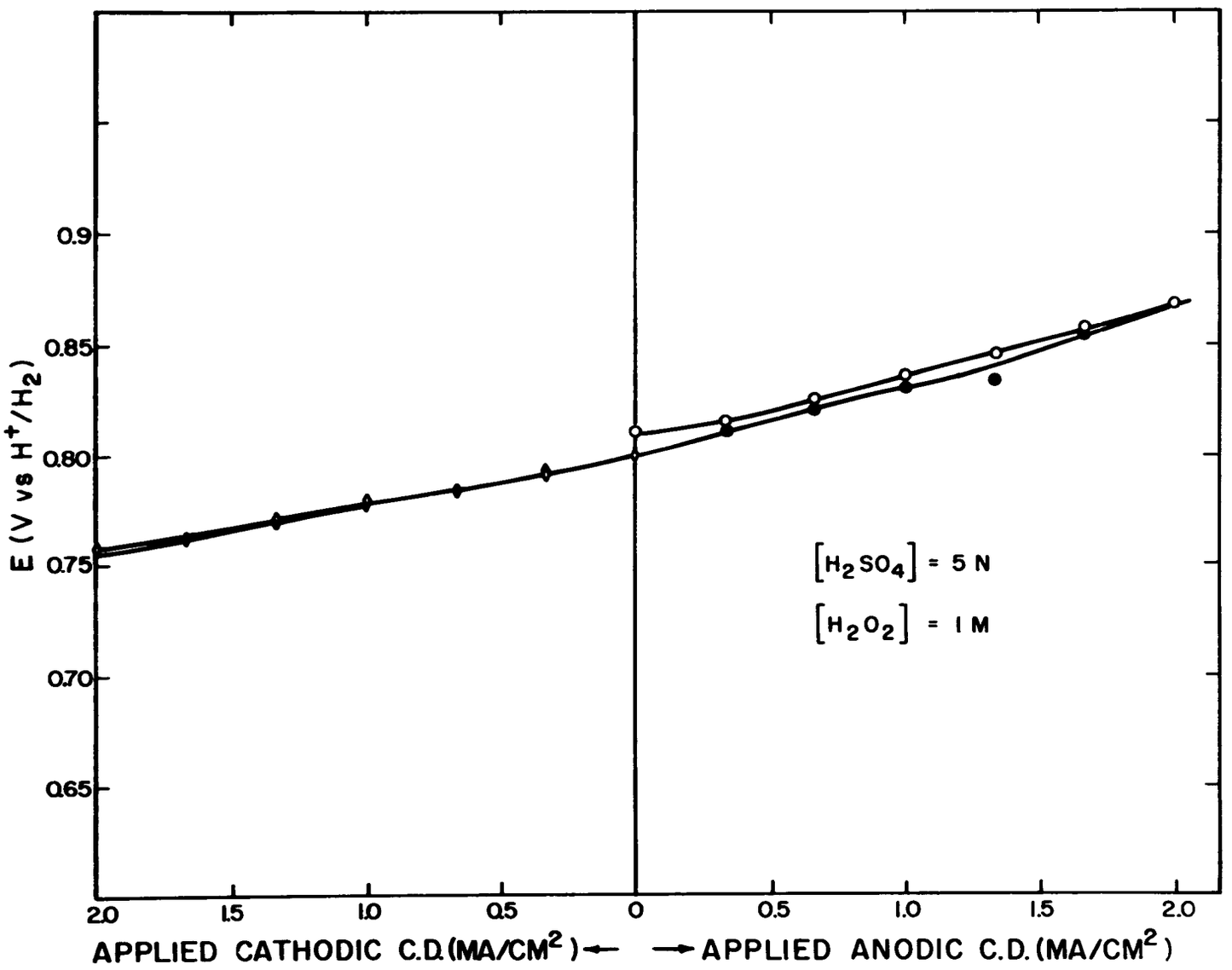
0.9
0.85
0.80
0.75
0.70
0.65
E (V vs H+/H2)
[H2SO4] = 5 N
[H2O2] = 1 M
2.0
1.5
1.0
0.5
0
0.5
1.0
1.5
2.0
APPLIED CATHODIC C.D.(MA/CM2) ← → APPLIED ANODIC C.D.(MA/CM2)

FIG. 11 e

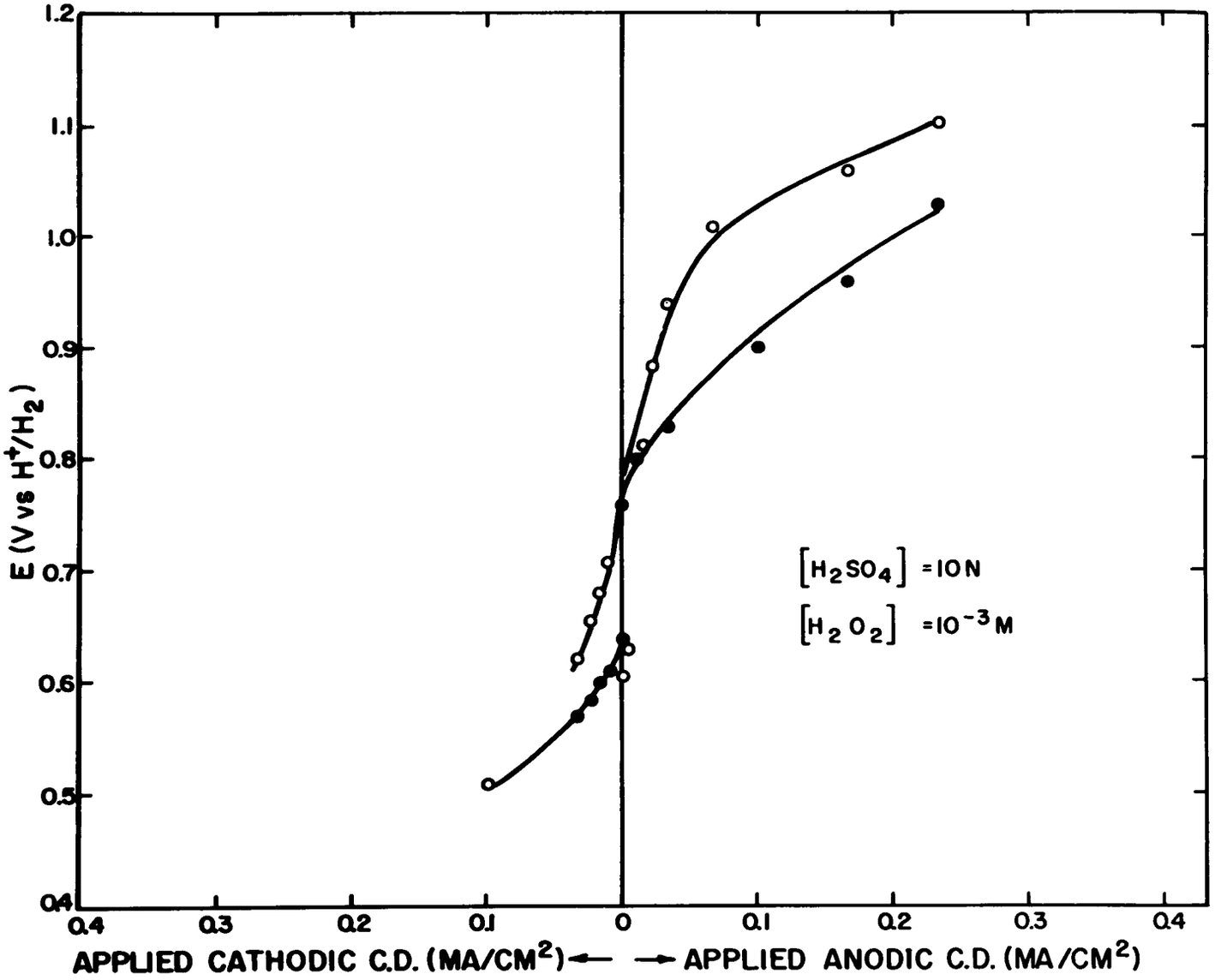
1.2
1.1
1.0
0.9
0.8
0.7
0.6
0.5
0.4
E (V vs H^+/H_2)
0.4
0.3
0.2
0.1
0
0.1
0.2
0.3
0.4
APPLIED CATHODIC C.D. (MA/CM^2) ← → APPLIED ANODIC C.D. (MA/CM^2)
$[H_2SO_4]$ = 10 N
$[H_2O_2]$ = 10^{-3} M

FIG. 11 f

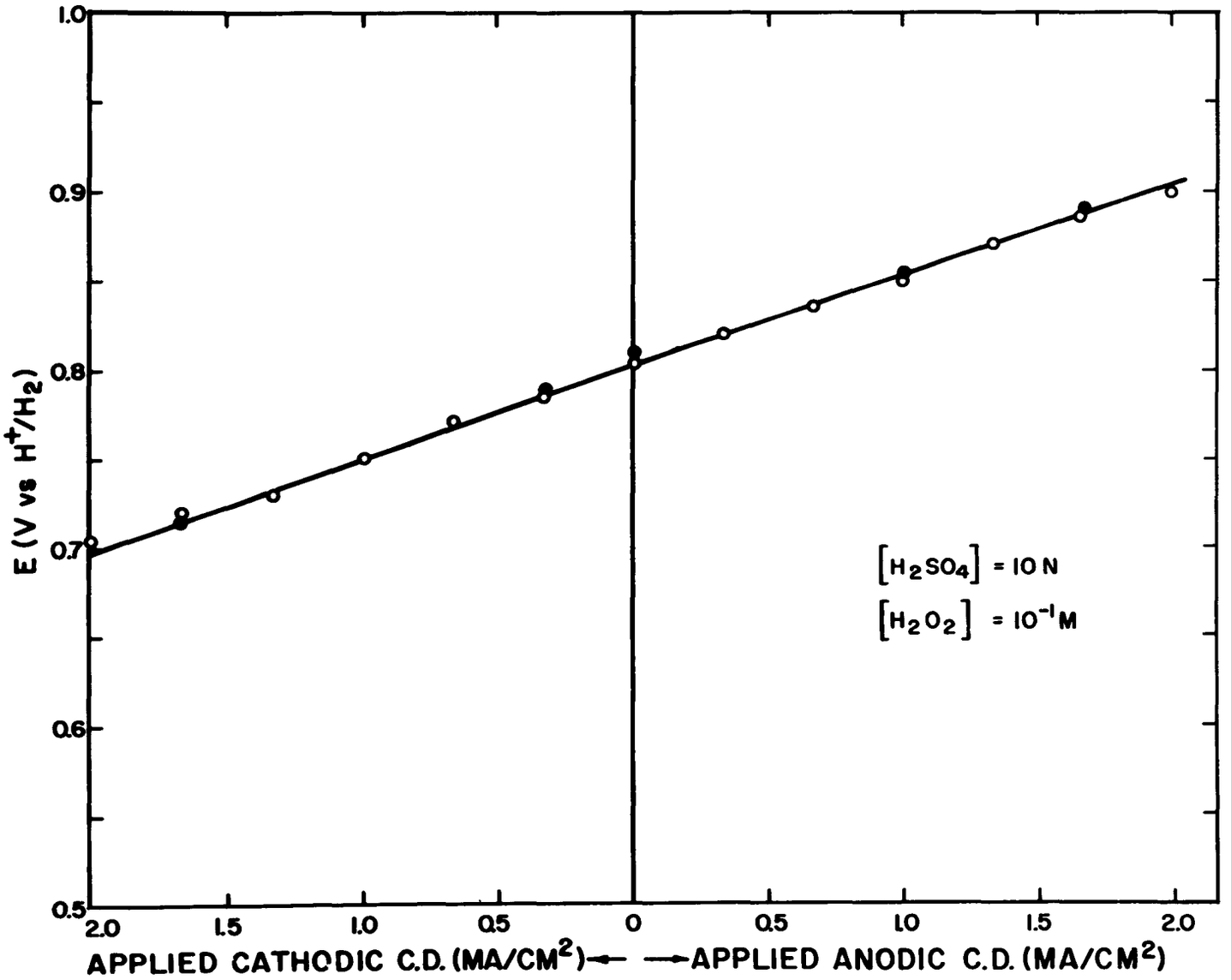
1.0
0.9
0.8
0.7
0.6
0.5
E (V vs H+/H2)
2.0
1.5
1.0
0.5
0
0.5
1.0
1.5
2.0
APPLIED CATHODIC C.D. (MA/CM2)
APPLIED ANODIC C.D. (MA/CM2)
[H2SO4] = 10 N
[H2O2] = 10-1 M

FIG. 11 g

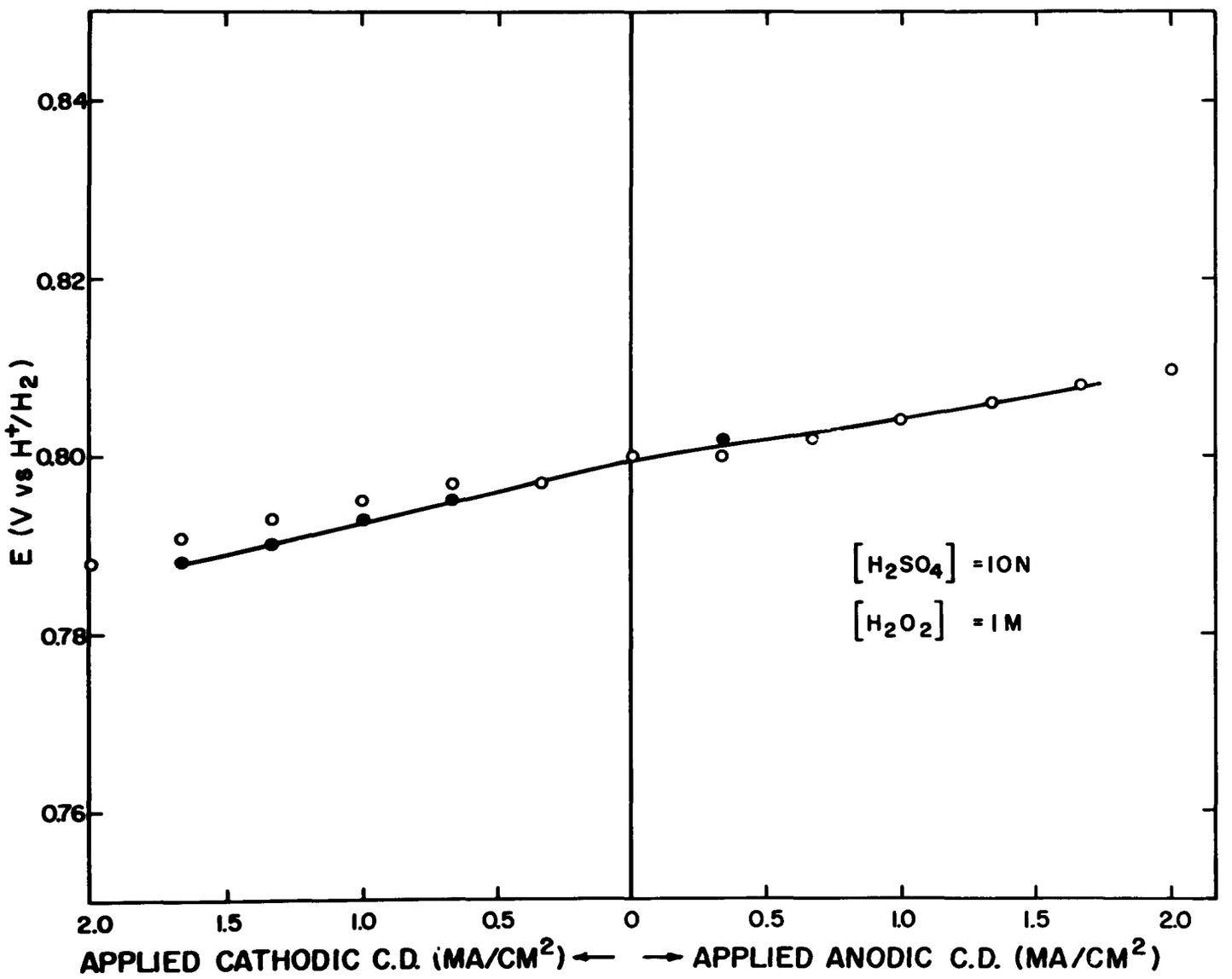
0.84
0.82
0.80
0.78
0.76
E (V vs H+/H2)
[H2SO4] = 10N
[H2O2] = 1M
2.0
1.5
1.0
0.5
0
0.5
1.0
1.5
2.0
APPLIED CATHODIC C.D. (MA/CM2) ← → APPLIED ANODIC C.D. (MA/CM2)

FIG. 11 h

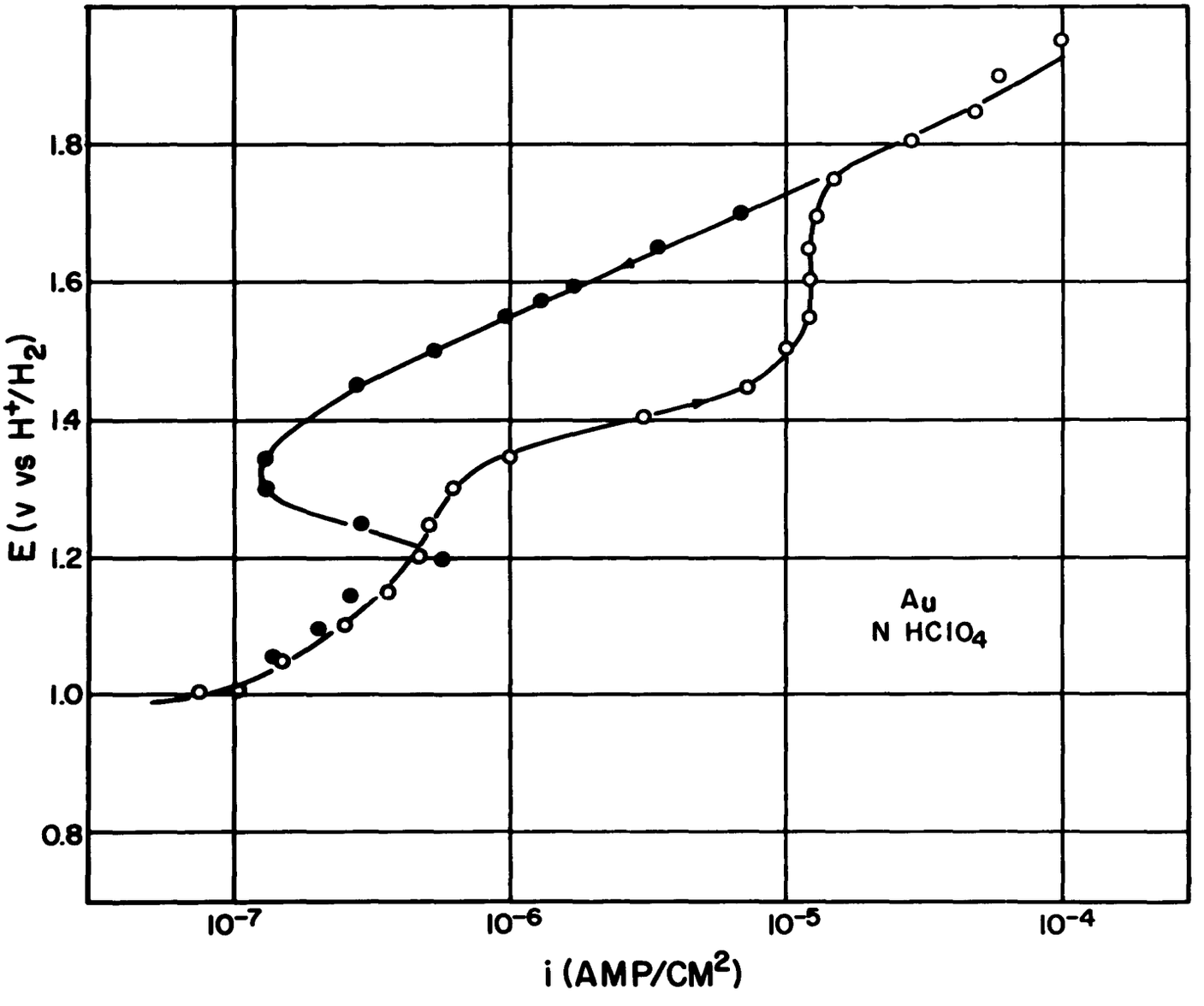

FIG. 12

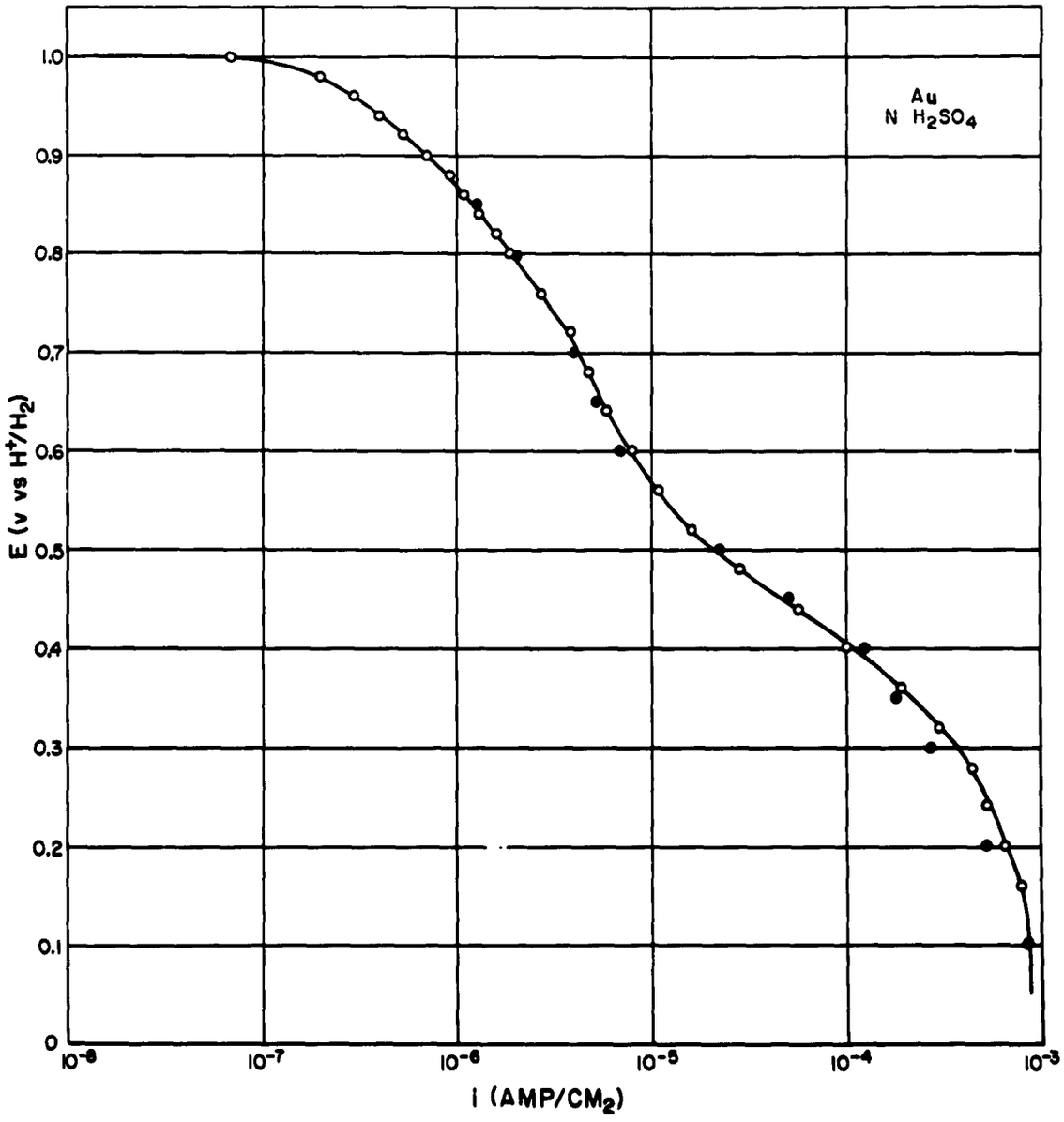
Au
N H_2SO_4
E (v vs H^+/H_2)
1.0
0.9
0.8
0.7
0.6
0.5
0.4
0.3
0.2
0.1
0
10^{-8}
10^{-7}
10^{-6}
10^{-5}
10^{-4}
10^{-3}
I (AMP/CM_2)

FIG. 13

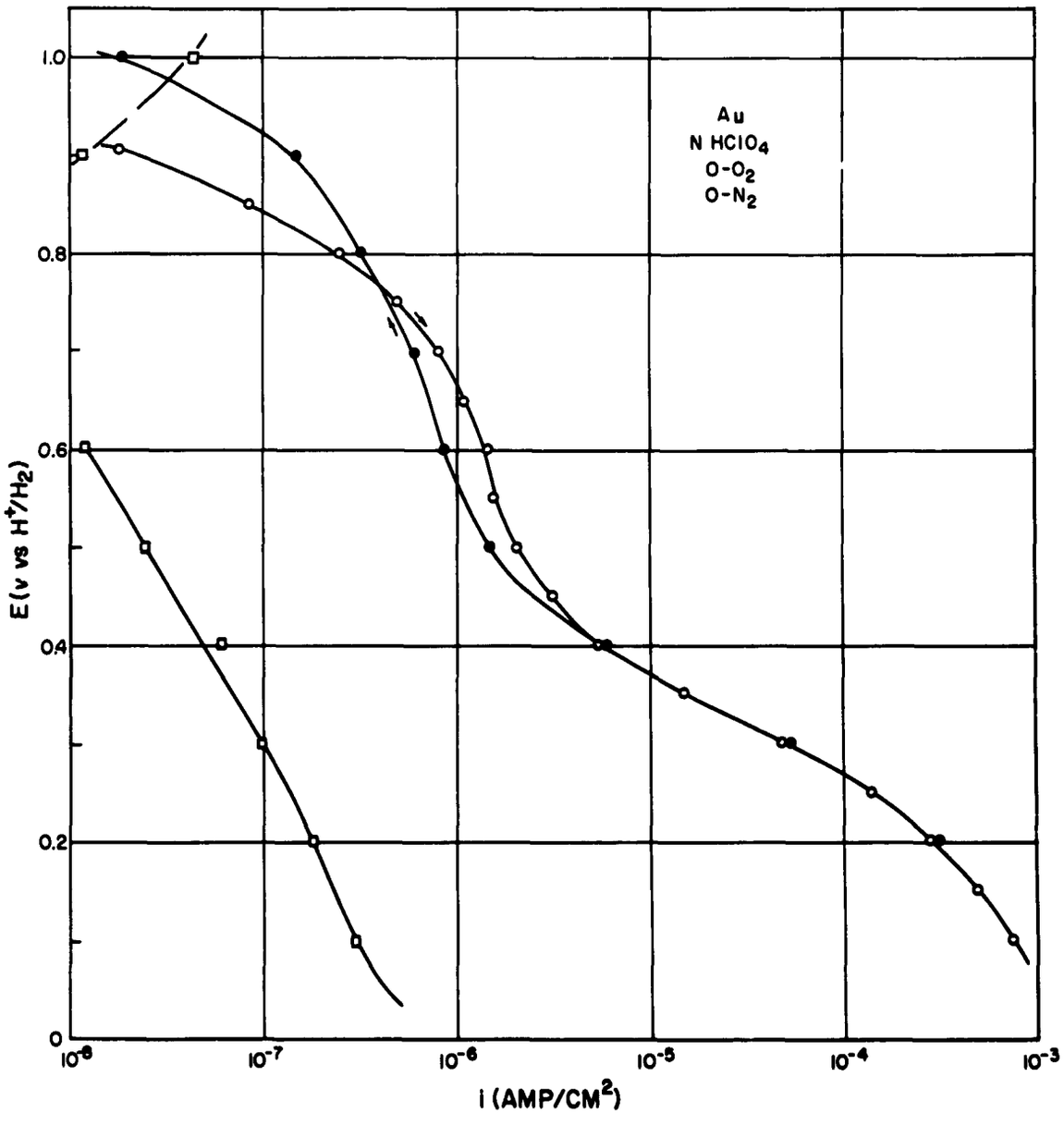
Au
N HClO4
O-O2
O-N2
1.0
0.8
0.6
0.4
0.2
0
E(v vs H+/H2)
10-8
10-7
10-6
10-5
10-4
10-3
i (AMP/CM2)

FIG. 14

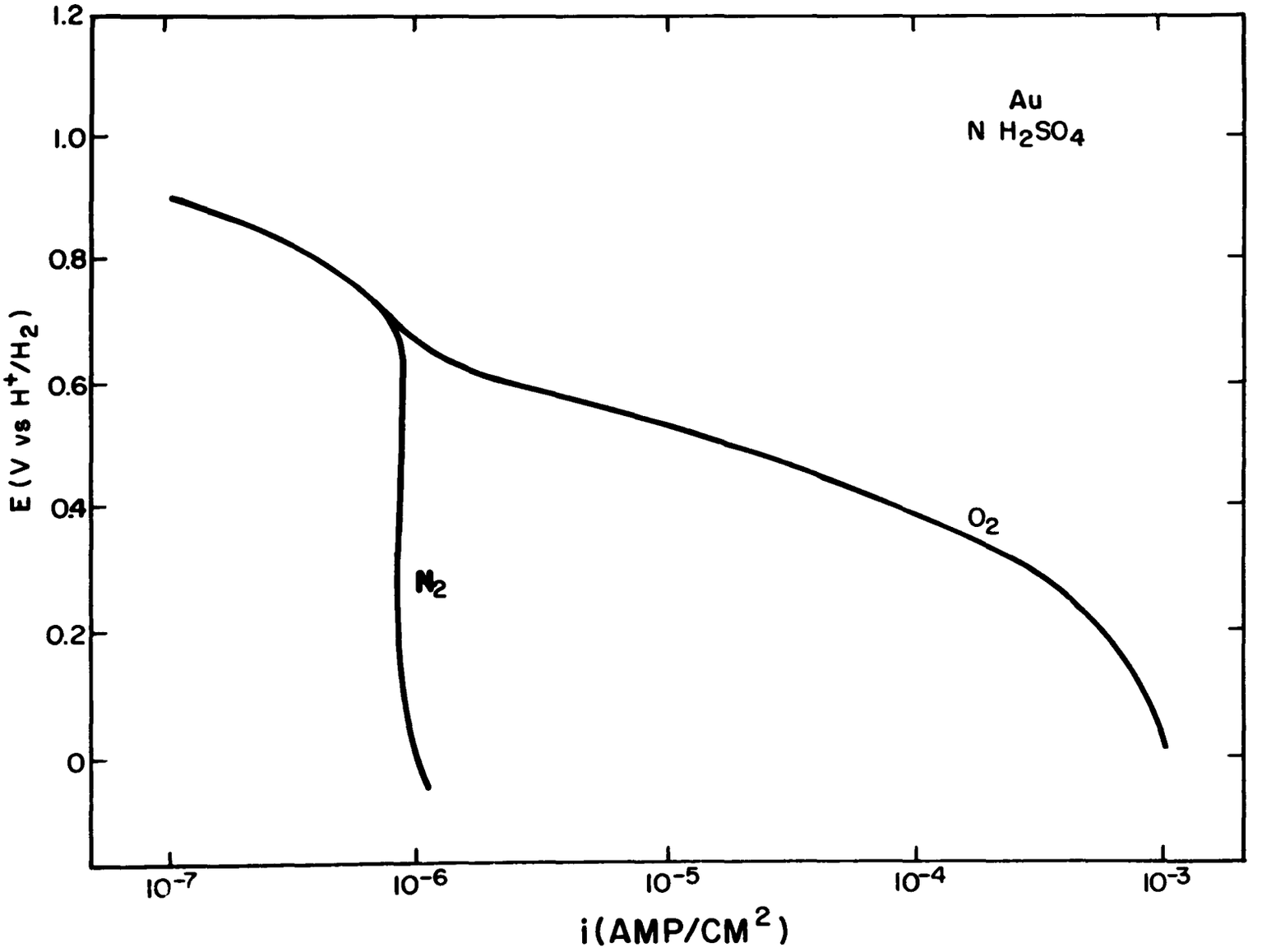
1.2
1.0
0.8
0.6
0.4
0.2
0
E (V vs H+/H2)
Au
N H2SO4
O2
N2
10-7
10-6
10-5
10-4
10-3
i(AMP/CM2)

FIG. 15

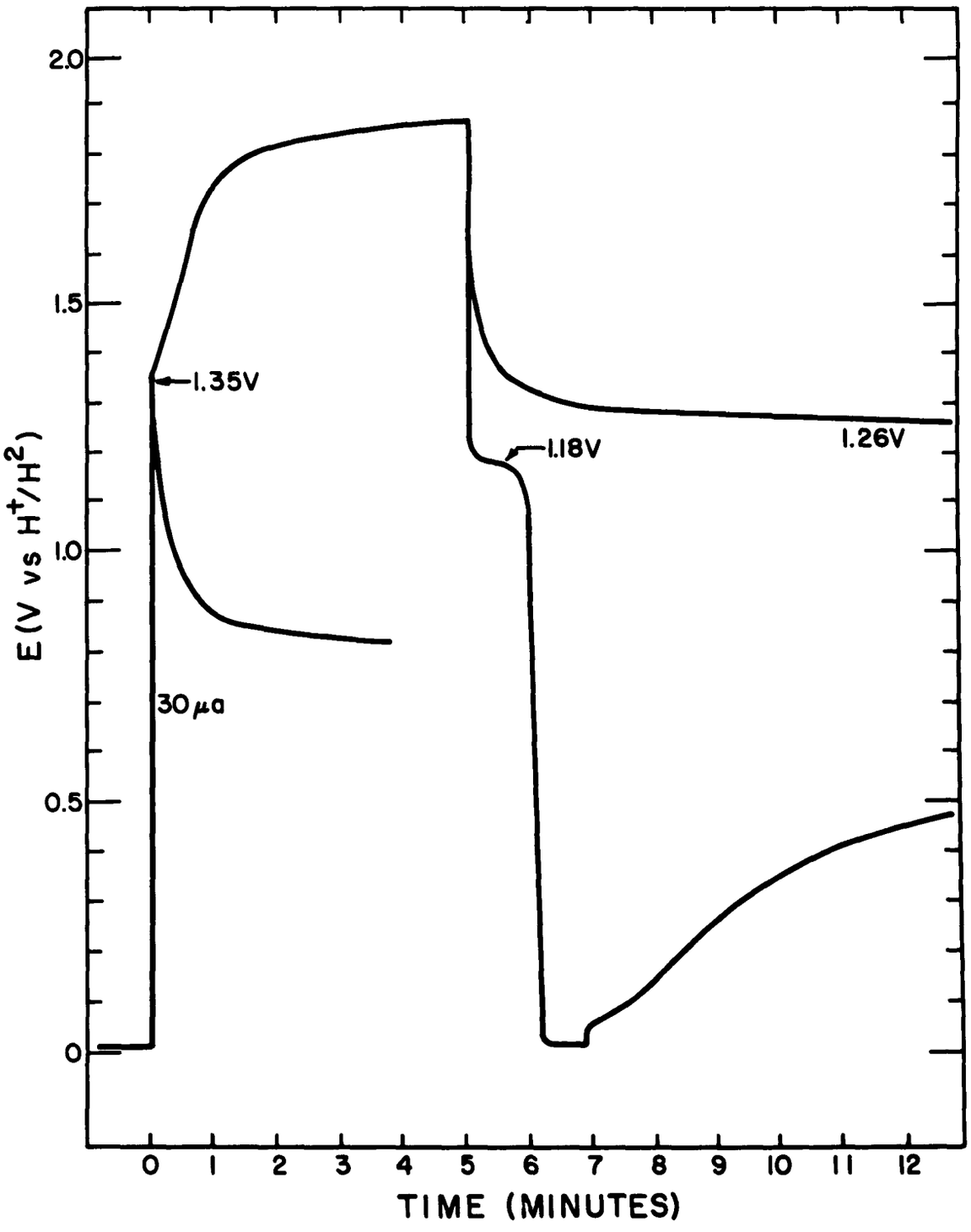
2.0
1.5
1.0
0.5
0
E (V vs H^+/H^2)
1.35V
1.18V
1.26V
30 μa
0 1 2 3 4 5 6 7 8 9 10 11 12
TIME (MINUTES)

FIG. 16

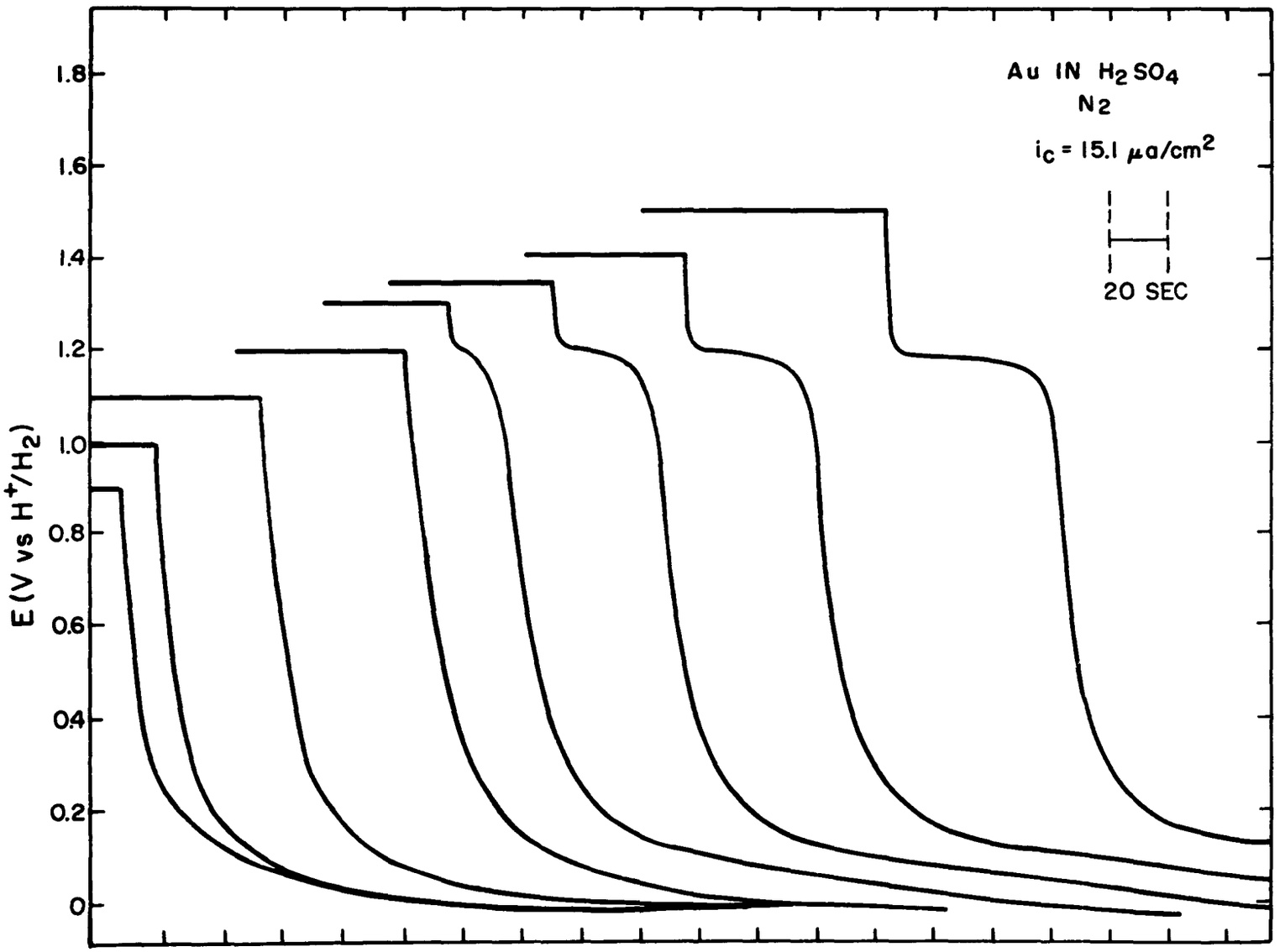
Au IN H_2SO_4
N_2
i_c = 15.1 μa/cm²
20 SEC
E (V vs H^+/H_2)
1.8
1.6
1.4
1.2
1.0
0.8
0.6
0.4
0.2
0

FIG. 17

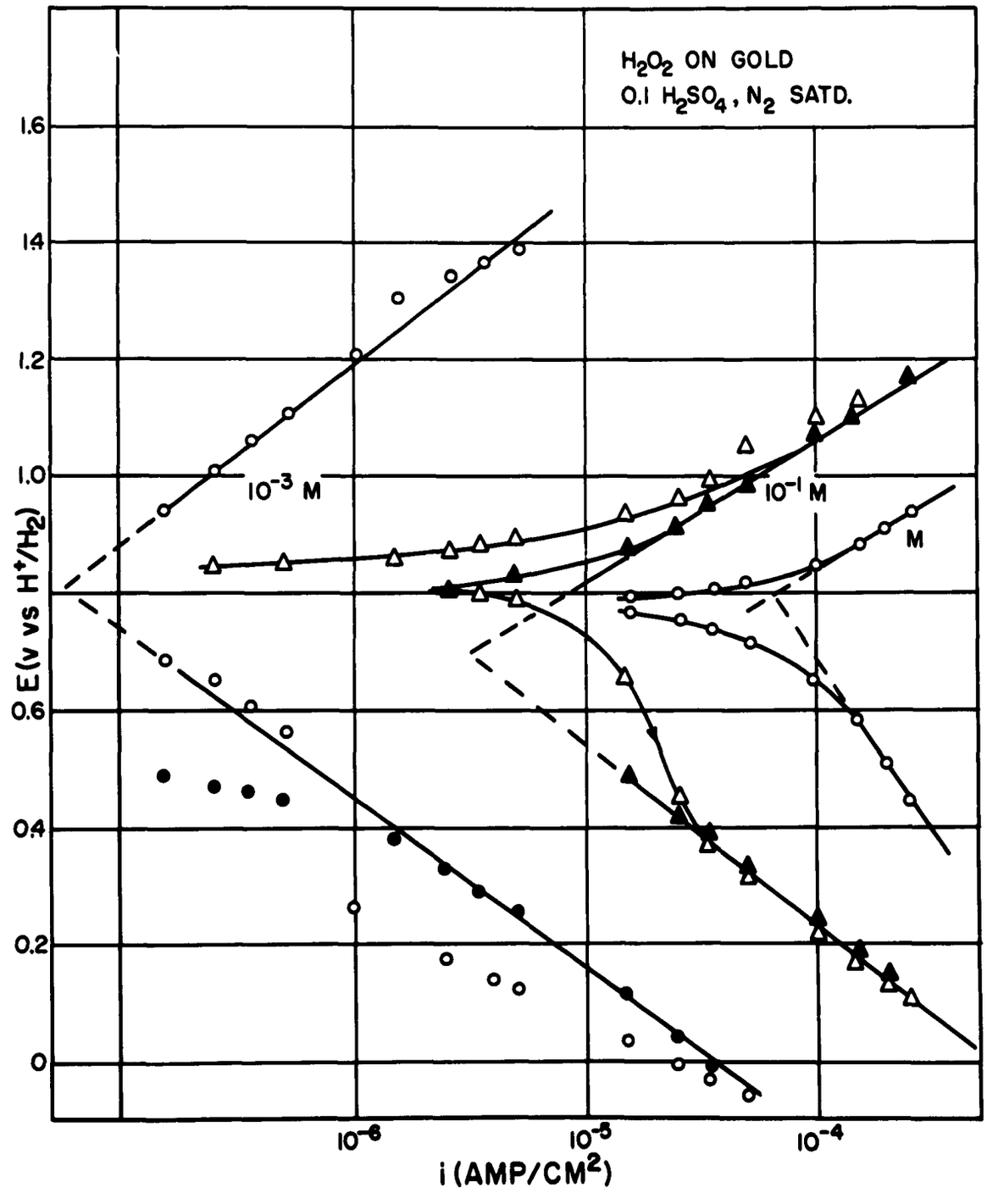
H_2O_2 ON GOLD
0.1 H_2SO_4, N_2 SATD.
1.6
1.4
1.2
1.0
0.6
0.4
0.2
0
E(v vs H^+/H_2)
10^{-3} M
10^{-1} M
M
10^{-6}
10^{-5}
10^{-4}
i (AMP/CM^2)

FIG. 18

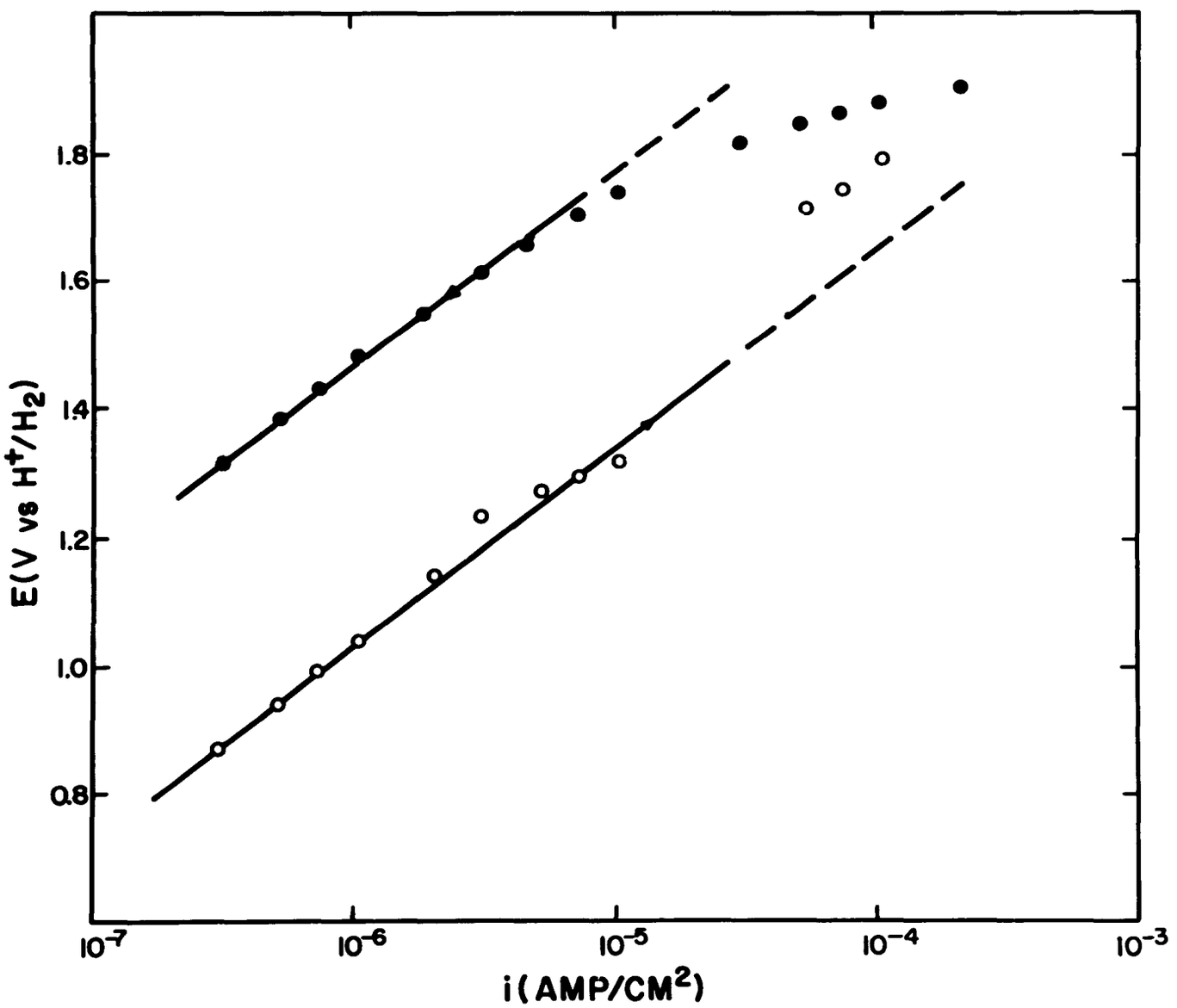

FIG. 19

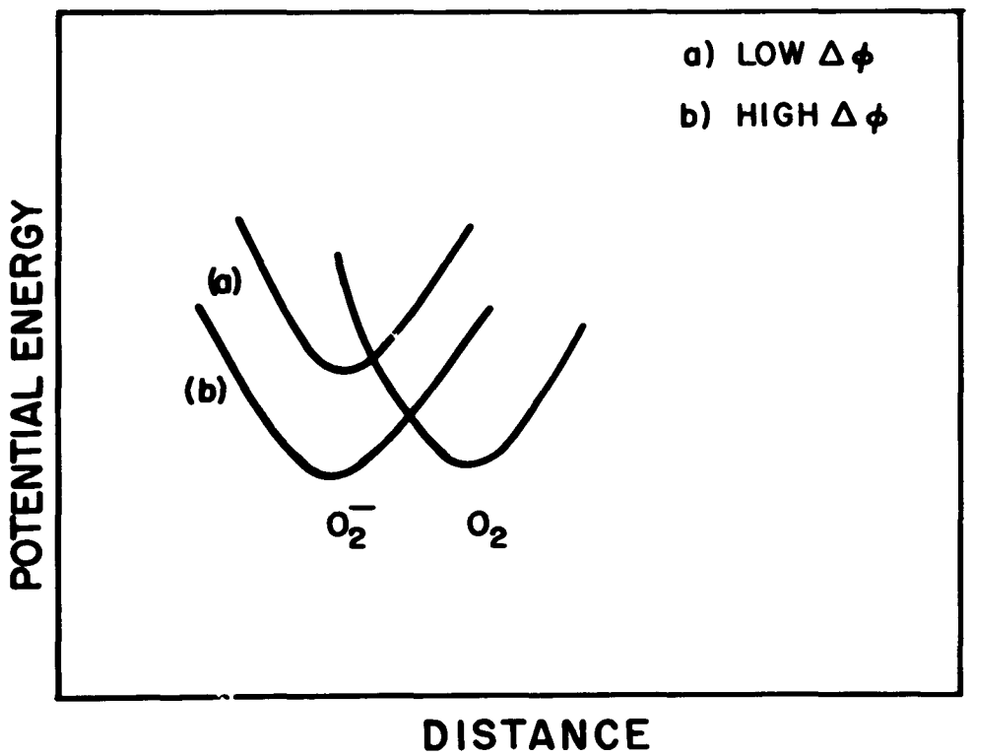

FIG. 20

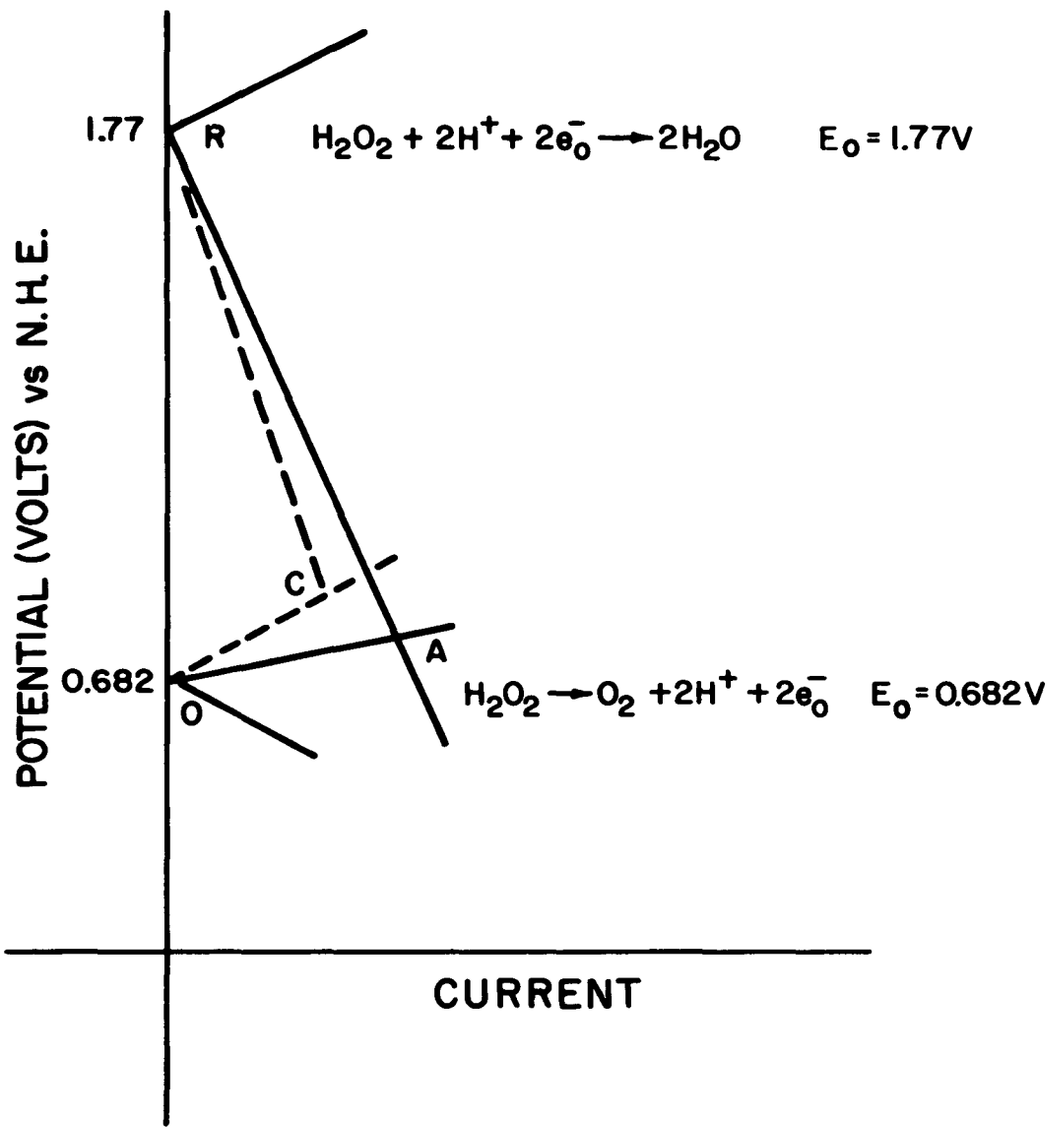
1.77
R
$H_2O_2 + 2H^+ + 2e_0^- \rightarrow 2H_2O$
$E_0 = 1.77V$
POTENTIAL (VOLTS) vs N.H.E.
C
A
0.682
O
$H_2O_2 \rightarrow O_2 + 2H^+ + 2e_0^-$
$E_0 = 0.682V$
CURRENT

FIG. 21

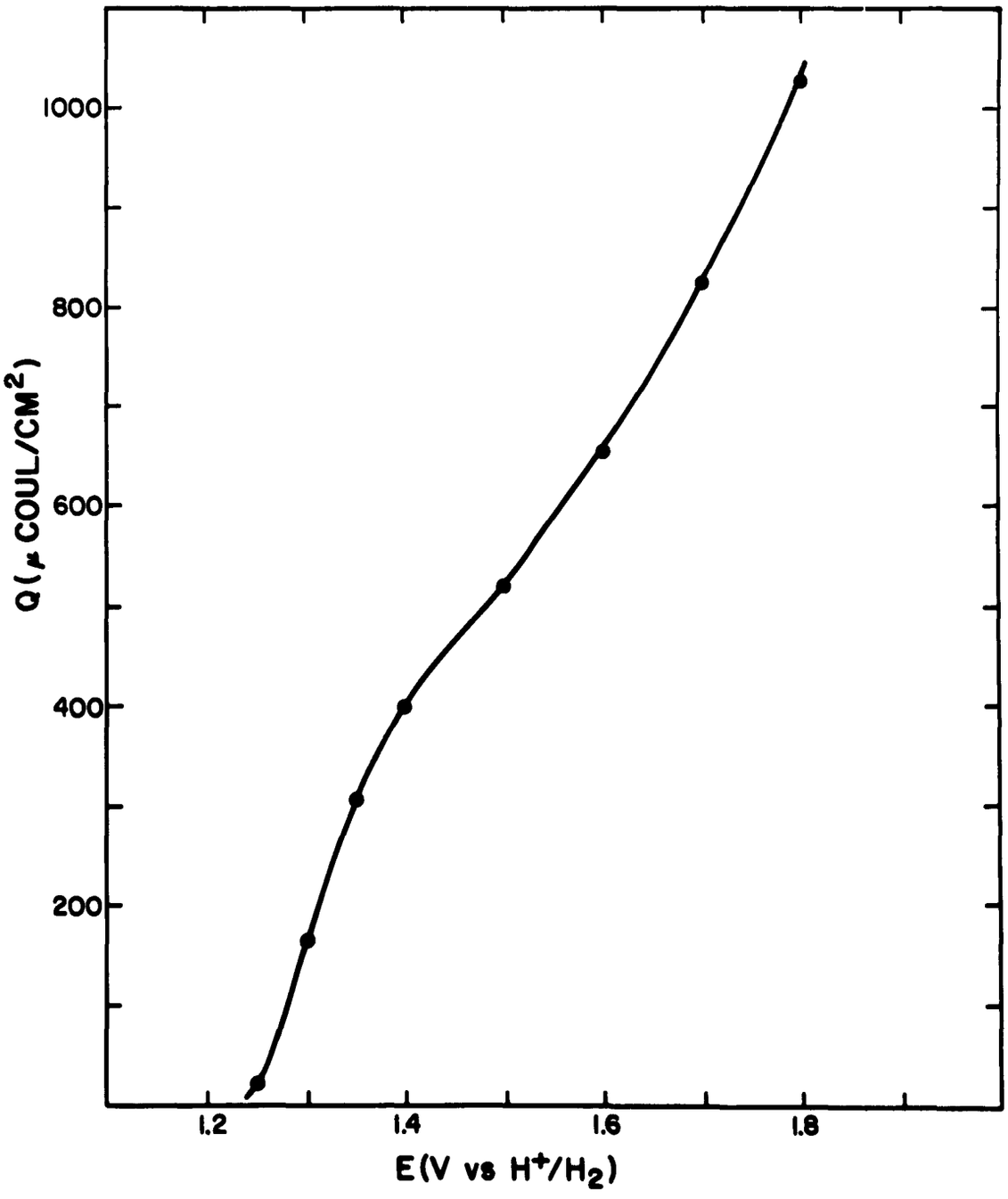

FIG. 22